

*Supplementary Information:*

**NALPS19: Sub-orbital scale climate variability recorded in Northern Alpine speleothems during the last glacial period**

Gina E. Moseley<sup>1</sup>, Christoph Spötl<sup>1</sup>, Susanne Brandstätter<sup>1</sup>, Tobias Erhardt<sup>2</sup>, Marc Luetscher<sup>1,4</sup>, R. Lawrence Edwards<sup>3</sup>

<sup>1</sup>Institute of Geology, University of Innsbruck, Innrain 52, 6020 Innsbruck, Austria

<sup>2</sup>Climate and Environmental Physics and Oeschger Center for Climate Change Research, University of Bern, Sidlerstrasse 5, 3012 Bern, Switzerland

<sup>3</sup>School of Earth Sciences, University of Minnesota, John T. Tate Hall, 116 Church Street SE, Minneapolis, MN 55455-0149, USA

<sup>4</sup>Swiss Institute for Speleology and Karst Studies (SISKA), 2301 La Chaux-de-Fonds, Switzerland

*Correspondence to:* Gina E. Moseley (gina.moseley@uibk.ac.at)



**GAS25**



**GAS27**



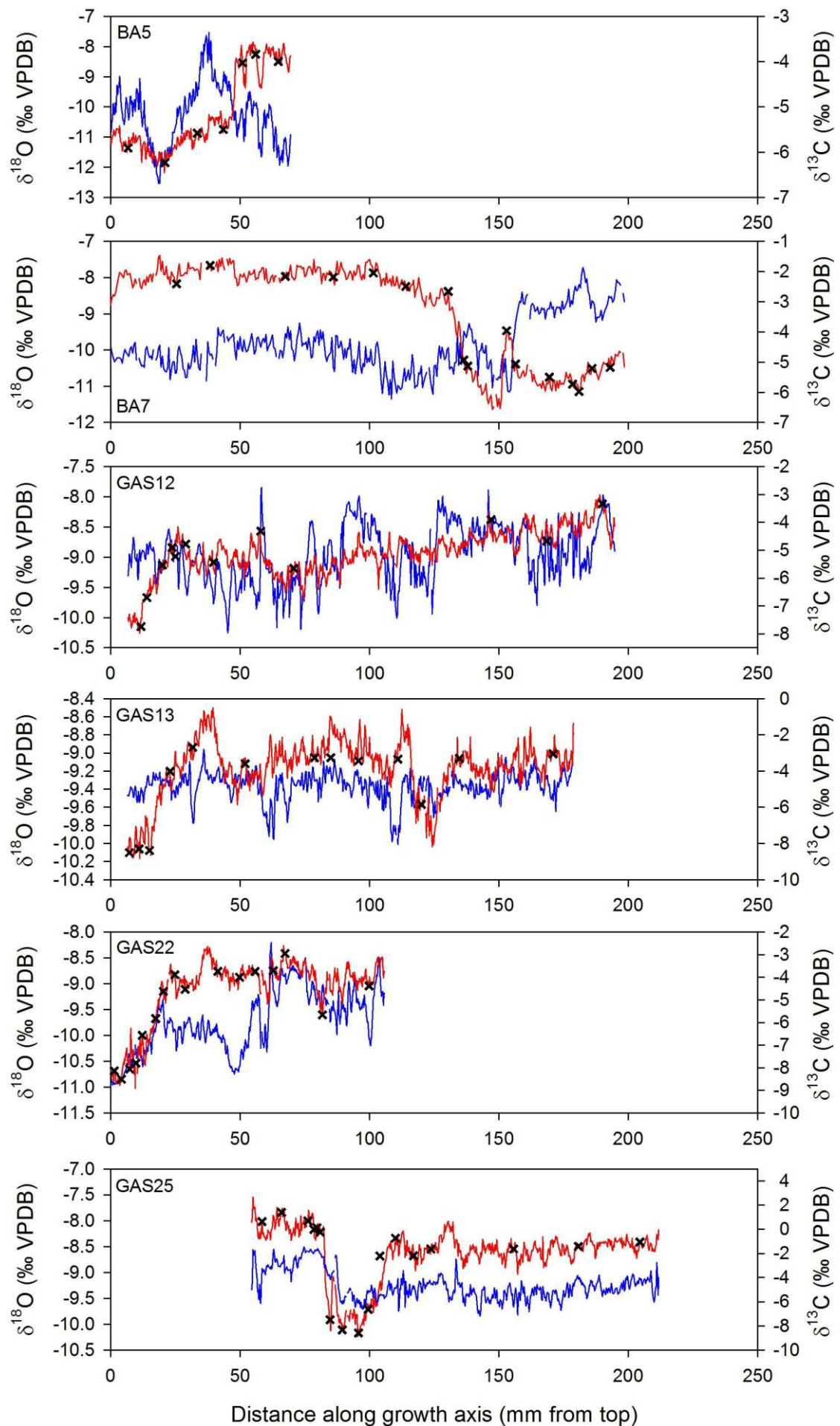
**GAS29**







**Figure S1: Samples analysed in this study. Black scale bars = 5cm.**





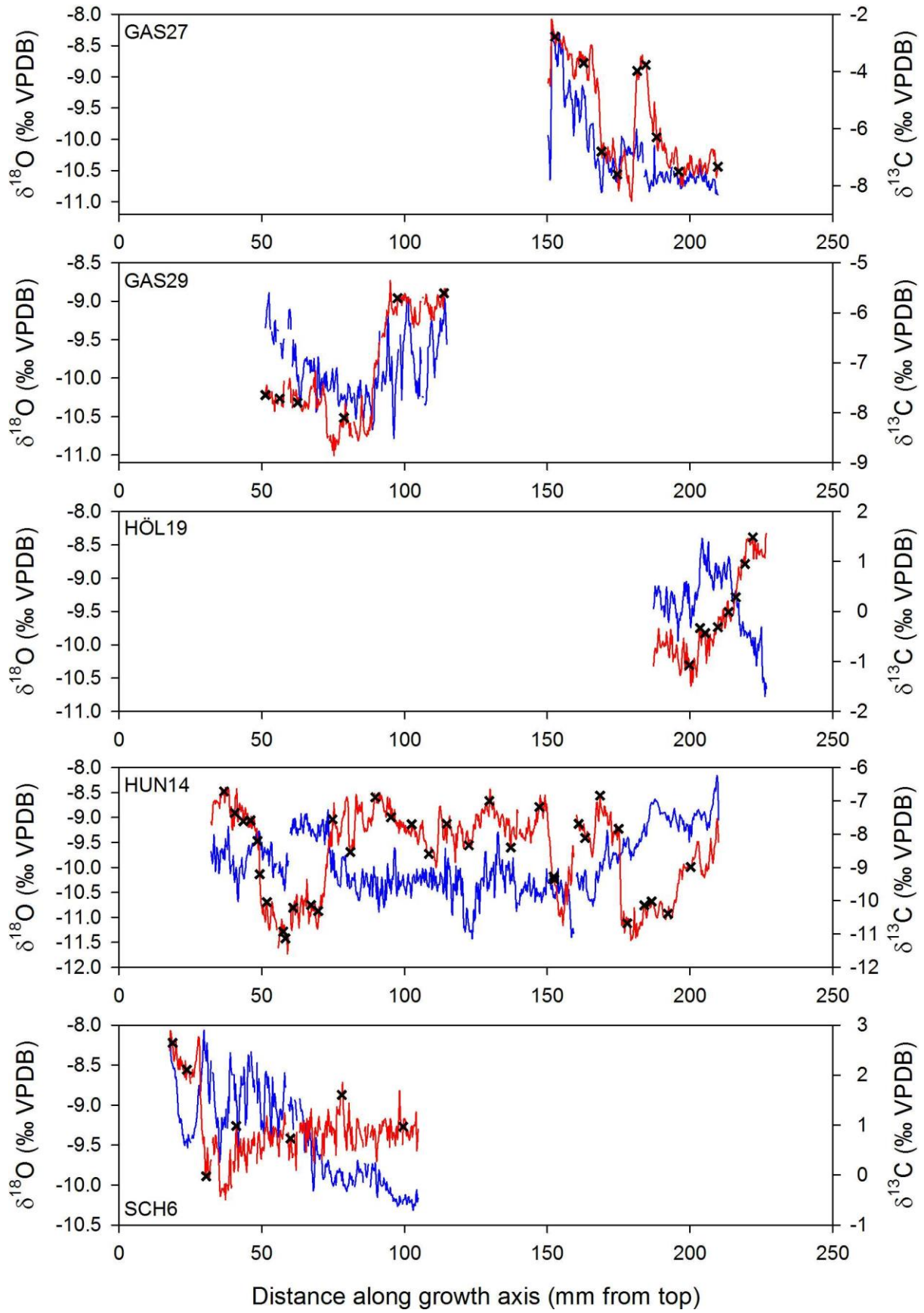


**Figure S2:**  $\delta^{18}\text{O}$  (red) and  $\delta^{13}\text{C}$  (blue) for each sample measured in this study relative to distance along growth axis. Black crosses mark locations of U-Th dating locations.

Sample (mm dft)	<sup>238</sup> U [ng g <sup>-1</sup> ]	<sup>232</sup> Th [pg g <sup>-1</sup> ]	<sup>230</sup> Th / <sup>232</sup> Th (atomic x10 <sup>-6</sup> )	δ <sup>234</sup> U* (measured)	<sup>230</sup> Th / <sup>238</sup> U† (activity)	Uncorrected Age (a)§	Corrected Age (a)#	δ <sup>234</sup> U* (initial)
<b>BA5</b>								
6.75	324 ± 0.3	941 ± 19	3,940 ± 80	249 ± 2	0.6939 ± 0.0014	85,513 ± 335	85,386 ± 337	316 ± 3
21.00	1085 ± 1.0	4,293 ± 86	2,900 ± 58	238 ± 2	0.6961 ± 0.0013	87,062 ± 300	86,909 ± 306	305 ± 2
33.50	287 ± 0.4	726 ± 15	4,503 ± 92	228 ± 2	0.6917 ± 0.0015	87,406 ± 368	87,286 ± 370	292 ± 3
43.50	295 ± 0.4	852 ± 17	3,911 ± 79	213 ± 2	0.6852 ± 0.0014	87,970 ± 361	87,841 ± 364	273 ± 3
51.00	1,174 ± 2	5,261 ± 106	2,508 ± 50	200 ± 2	0.6819 ± 0.0015	88,901 ± 405	88,733 ± 411	257 ± 3
56.00	312 ± 0.4	1,814 ± 36	1,943 ± 39	201 ± 2	0.6854 ± 0.0013	89,380 ± 334	89,183 ± 346	259 ± 2
64.75	331 ± 0.4	1,015 ± 20	3,681 ± 74	192 ± 2	0.6838 ± 0.0015	90,195 ± 384	90,060 ± 387	248 ± 3
<b>BA7</b>								
25.50	785 ± 0.9	2,764 ± 55	3,473 ± 70	365 ± 1	0.7416 ± 0.0012	81,844 ± 230	81,707 ± 235	460 ± 2
38.50	378 ± 0.4	55,427 ± 1,110	85 ± 2	372 ± 2	0.7592 ± 0.0017	83,987 ± 330	80,985 ± 2,107	468 ± 4
67.50	805 ± 1.0	7,239 ± 145	1,371 ± 28	364 ± 2	0.7482 ± 0.0014	83,011 ± 289	82,769 ± 315	460 ± 3
86.00	718 ± 0.8	20,457 ± 410	434 ± 9	359 ± 2	0.7491 ± 0.0012	83,637 ± 258	82,999 ± 479	454 ± 2
101.50	1411 ± 1.8	50,860 ± 1,019	344 ± 7	356 ± 2	0.7514 ± 0.0015	84,280 ± 308	83,491 ± 597	451 ± 2
114.00	751 ± 0.8	98,543 ± 1,973	96 ± 2	349 ± 2	0.7613 ± 0.0013	86,576 ± 267	83,831 ± 1,914	443 ± 3
130.50	718 ± 1.1	135,400 ± 2,715	66 ± 1	339 ± 2	0.7555 ± 0.0017	86,676 ± 338	82,705 ± 2786	428 ± 4
136.50	610 ± 0.7	39,611 ± 793	190 ± 4	330 ± 1	0.7466 ± 0.0012	86,077 ± 242	84,671 ± 977	419 ± 2
138.00	634 ± 0.9	62,210 ± 1,247	126 ± 3	34 ± 2	0.7526 ± 0.0016	86,711 ± 336	84,625 ± 1469	424 ± 3
153.00	584 ± 0.6	34,428 ± 689	208 ± 4	327 ± 2	0.7442 ± 0.0014	85,954 ± 279	84,670 ± 904	416 ± 2
156.50	566 ± 0.6	22,531 ± 451	311 ± 6	333 ± 1	0.7497 ± 0.0012	86,288 ± 251	85,405 ± 628	424 ± 2
169.50	600 ± 0.7	27,111 ± 543	274 ± 5	321 ± 2	0.7492 ± 0.0014	87,421 ± 323	76,423 ± 735	410 ± 3
178.50	600 ± 0.6	13,016 ± 261	567 ± 11	322 ± 2	0.7459 ± 0.0013	86,750 ± 281	86,240 ± 423	411 ± 2
181.00	720 ± 0.9	9,246 ± 185	955 ± 19	320 ± 2	0.7433 ± 0.0013	86,617 ± 280	86,284 ± 336	408 ± 2
186.00	507 ± 0.6	19,718 ± 395	318 ± 6	318 ± 2	0.7494 ± 0.0014	87,801 ± 360	86,932 ± 673	407 ± 3
193.00	444 ± 0.5	62,846 ± 1,259	89 ± 2	310 ± 1	0.7629 ± 0.0014	91,076 ± 303	88,022 ± 2,136	398 ± 3
<b>HÖL19</b>								
7.25	435 ± 0.5	29,311 ± 587	10 ± 0.2	-73 ± 2	0.0417 ± 0.0005	5,028 ± 57	3,864 ± 591	-74 ± 2
<i>Hiatus</i>								
76.00	467 ± 0.4	3,901 ± 78	249 ± 5	-30 ± 1	0.1261 ± 0.0004	15,195 ± 55	14,998 ± 88	-31 ± 1
81.00	1,605 ± 2	1,598 ± 32	2,022 ± 41	-57 ± 1	0.1221 ± 0.0002	15,141 ± 36	15,058 ± 37	-59 ± 1
97.25	985 ± 1	1,504 ± 30	1,383 ± 28	-47 ± 1	0.1280 ± 0.0002	15,748 ± 38	15,657 ± 40	-49 ± 1
<i>Hiatus</i>								
178.50	446 ± 0.5	1,437 ± 29	2,203 ± 44	-84 ± 1	0.4305 ± 0.0008	70,028 ± 253	69,912 ± 255	-102 ± 2
<i>Hiatus</i>								
ISOCHRON age for 199.75mm				-105 ± 2	0.4346 ± 0.0014	73,720 ± 410	73,656 ± 410	-129 ± 2

Sample (mm dft)	$^{238}\text{U}$ [ng g <sup>-1</sup> ]	$^{232}\text{Th}$ [pg g <sup>-1</sup> ]	$^{230}\text{Th} / ^{232}\text{Th}$ (atomic x10 <sup>-6</sup> )	$\delta^{234}\text{U}^*$ (measured)	$^{230}\text{Th} / ^{238}\text{U}^\dagger$ (activity)	Uncorrected Age (a)§	Corrected Age (a)#	$\delta^{234}\text{U}^*$ (initial)
<b><u>HÖL19</u></b>								
203.50	777 ± 1	2,736 ± 55	2,034 ± 41	-108 ± 1	0.4346 ± 0.0009	74,156 ± 300	74,032 ± 302	-134 ± 2
205.25	822 ± 1	1,964 ± 39	2,982 ± 60	-113 ± 1	0.4322 ± 0.0010	74,140 ± 292	74,031 ± 292	-139 ± 2
209.75	759 ± 1	4,104 ± 82	1,327 ± 27	-108 ± 1	0.4348 ± 0.0009	74,127 ± 298	73,970 ± 301	-133 ± 2
213.50	603 ± 1	5,058 ± 101	861 ± 17	-106 ± 1	0.4381 ± 0.0010	74,671 ± 315	74,459 ± 324	-131 ± 2
216.00	492 ± 1	4,260 ± 85	832 ± 17	-104 ± 1	0.4368 ± 0.0009	74,072 ± 290	73,859 ± 300	-128 ± 2
219.25	674 ± 1	5,186 ± 104	939 ± 19	-106 ± 2	0.4379 ± 0.0012	74,638 ± 373	74,441 ± 379	-131 ± 2
222.00	648 ± 1	2,057 ± 41	2,261 ± 45	-109 ± 1	0.4356 ± 0.0009	74,426 ± 284	74,303 ± 285	-134 ± 2
<i>Hiatus</i>								
394.00	851 ± 1	54,302 ± 1,088	128 ± 3	-61 ± 2	0.4959 ± 0.0011	82,747 ± 429	81,638 ± 700	-77 ± 3
<b><u>SCH6</u></b>								
11.25	166 ± 0.2	27,618 ± 553	70 ± 1	382 ± 2	0.7071 ± 0.0035	75,074 ± 529	71,664 ± 2,424	468 ± 4
<i>Hiatus</i>								
18.75	54 ± 0.04	2,294 ± 46	301 ± 6	493 ± 2	0.7689 ± 0.0020	75,275 ± 304	74,443 ± 520	608 ± 3
23.75	66 ± 0.05	1,979 ± 40	428 ± 9	499 ± 2	0.7785 ± 0.0017	76,077 ± 263	75,469 ± 463	618 ± 2
30.50	166 ± 0.11	584 ± 12	3,757 ± 76	543 ± 1	0.8022 ± 0.0014	76,024 ± 214	75,896 ± 218	673 ± 2
41.00	269 ± 0.30	267 ± 5	13,477 ± 278	551 ± 2	0.8110 ± 0.0012	76,544 ± 211	76,460 ± 211	684 ± 2
60.00	259 ± 0.24	793 ± 16	4,375 ± 88	548 ± 2	0.8131 ± 0.0012	77,081 ± 198	76,961 ± 202	681 ± 2
78.00	209 ± 0.20	502 ± 10	5,594 ± 113	546 ± 2	0.8145 ± 0.0013	77,430 ± 220	77,321 ± 222	679 ± 2
99.50	222 ± 0.21	575 ± 12	5,182 ± 105	538 ± 2	0.8148 ± 0.0012	78,038 ± 204	77,926 ± 206	670 ± 2
<b><u>HUN14</u></b>								
36.75	576 ± 0.6	1,126 ± 23	6,842 ± 138	288 ± 1	0.8107 ± 0.0011	102,942 ± 297	102,834 ± 298	385 ± 2
40.50	673 ± 2	1,279 ± 7	6,854 ± 36	255 ± 1	0.7899 ± 0.0012	103,443 ± 312	103,335 ± 313	341 ± 2
43.50	534 ± 0.6	1,280 ± 26	5,446 ± 110	256 ± 2	0.7921 ± 0.0014	103,770 ± 402	103,654 ± 404	343 ± 2
45.50	389 ± 0.4	1,455 ± 29	3,426 ± 69	233 ± 2	0.7774 ± 0.0013	104,030 ± 376	103,883 ± 380	312 ± 2
48.50	468 ± 1	635 ± 4	9,156 ± 47	201 ± 1	0.7537 ± 0.0007	103,732 ± 242	103,634 ± 243	269 ± 2
49.25	365 ± 0.3	873 ± 18	5,278 ± 107	187 ± 1	0.7457 ± 0.0010	104,093 ± 326	103,971 ± 328	251 ± 2
51.75	413 ± 0.5	512 ± 10	110,443 ± 212	243 ± 2	0.7849 ± 0.0014	104,095 ± 391	104,004 ± 391	326 ± 2
57.50	555 ± 1	479 ± 3	14,456 ± 77	205 ± 1	0.7570 ± 0.0008	103,803 ± 298	103,717 ± 299	275 ± 2
58.25	536 ± 0.5	301 ± 6	22,112 ± 462	195 ± 1	0.7526 ± 0.0010	104,357 ± 310	104,277 ± 310	262 ± 2
<i>Hiatus</i>								
61.00	315 ± 0.3	787 ± 16	4910 ± 101	174 ± 2	0.7440 ± 0.0016	105,787 ± 490	105,664 ± 491	235 ± 3
67.50	250 ± 0.2	413 ± 8	7893 ± 161	241 ± 2	0.7909 ± 0.0012	105,718 ± 345	105,617 ± 346	325 ± 2
69.75	349 ± 0.3	547 ± 11	8,612 ± 174	282 ± 1	0.8201 ± 0.0010	105,732 ± 301	105,632 ± 302	380 ± 2
74.75	494 ± 0.6	266 ± 5	25,249 ± 522	286 ± 2	0.8232 ± 0.0015	105,895 ± 391	105,820 ± 391	385 ± 2



Sample (mm dft)	$^{238}\text{U}$ [ng g <sup>-1</sup> ]	$^{232}\text{Th}$ [pg g <sup>-1</sup> ]	$^{230}\text{Th} / ^{232}\text{Th}$ (atomic x10 <sup>-6</sup> )	$\delta^{234}\text{U}^*$ (measured)	$^{230}\text{Th} / ^{238}\text{U}^\dagger$ (activity)	Uncorrected Age (a)§	Corrected Age (a)#	$\delta^{234}\text{U}^*$ (initial)
<b>HUN14</b>								
81.00	455 ± 0.6	1,146 ± 23	5,595 ± 113	327 ± 2	0.8553 ± 0.0016	106,486 ± 402	106,371 ± 404	441 ± 2
89.75	570 ± 0.7	296 ± 7	27,371 ± 615	339 ± 2	0.8624 ± 0.0017	106,231 ± 442	106,156 ± 442	457 ± 3
95.25	720 ± 2	446 ± 3	22,289 ± 120	301 ± 2	0.8366 ± 0.0010	106,473 ± 316	106,393 ± 315	406 ± 2
102.50	957 ± 1	153 ± 4	84,773 ± 1,949	283 ± 2	0.8238 ± 0.0013	106,391 ± 381	106,320 ± 381	382 ± 2
108.50	449 ± 0.5	127 ± 3	48,120 ± 1,121	277 ± 2	0.8232 ± 0.0014	107,081 ± 374	107,010 ± 374	375 ± 2
115.00	612 ± 0.6	250 ± 5	33,598 ± 708	289 ± 1	0.8313 ± 0.0013	107,121 ± 343	107,049 ± 343	391 ± 2
122.50	824 ± 2	331 ± 2	33,927 ± 192	282 ± 2	0.8261 ± 0.0011	106,950 ± 353	106,874 ± 353	382 ± 2
129.75	407 ± 0.4	117 ± 3	47,557 ± 1,086	281 ± 2	0.8273 ± 0.0013	107,420 ± 366	107,350 ± 366	381 ± 2
137.25	560 ± 0.4	695 ± 14	10,684 ± 216	250 ± 1	0.8047 ± 0.0010	107,297 ± 315	107,202 ± 316	339 ± 2
147.25	622 ± 0.6	97 ± 2	82,601 ± 1,299	213 ± 1	0.7772 ± 0.0013	107,138 ± 375	107,071 ± 375	288 ± 2
152.25	742 ± 0.7	230 ± 1	40,716 ± 224	192 ± 1	0.7642 ± 0.0011	107,585 ± 331	107,514 ± 331	260 ± 2
152.50	524 ± 0.5	324 ± 7	20,374 ± 425	191 ± 1	0.7633 ± 0.0010	107,415 ± 338	107,333 ± 338	259 ± 2
<i>Hiatus</i>								
161.00	708 ± 2	1,336 ± 27	6,760 ± 139	203 ± 2	0.7733 ± 0.0026	107,867 ± 910	107,757 ± 910	275 ± 3
163.25	692 ± 0.5	1,051 ± 21	8,375 ± 169	200 ± 1	0.7719 ± 0.0009	108,107 ± 309	108,004 ± 310	270 ± 2
168.50	519 ± 0.3	2,001 ± 40	3,299 ± 66	195 ± 1	0.7707 ± 0.0010	108,513 ± 315	108,356 ± 321	265 ± 2
175.00	572 ± 1	1,244 ± 25	5,644 ± 115	157 ± 2	0.7442 ± 0.0025	108,796 ± 702	108,676 ± 703	213 ± 3
178.00	1,398 ± 1	1,542 ± 31	11,118 ± 223	156 ± 1	0.7435 ± 0.0011	108,818 ± 361	108,727 ± 361	212 ± 2
184.00	769 ± 1	764 ± 16	12,389 ± 254	157 ± 2	0.7469 ± 0.0016	109,375 ± 487	109,287 ± 488	214 ± 2
186.50	786 ± 2	1,846 ± 37	5477 ± 111	200 ± 2	0.7808 ± 0.0023	110,128 ± 647	110,007 ± 648	272 ± 3
192.25	820 ± 0.8	725 ± 15	15,299 ± 309	252 ± 2	0.8201 ± 0.0012	110,453 ± 367	110,370 ± 367	344 ± 2
200.25	1,307 ± 1	1,468 ± 29	12,456 ± 251	290 ± 2	0.8490 ± 0.0013	110,643 ± 378	110,556 ± 378	397 ± 2
<b>GAS12</b>								
11.75	344 ± 0.7	21 ± 6	152,718 ± 48,200	82 ± 3	0.5539 ± 0.0029	77,363 ± 659	77,303 ± 659	102 ± 3
14.00	389 ± 0.5	26 ± 2	139,450 ± 8,216	87 ± 2	0.5561 ± 0.0011	77,151 ± 285	77,085 ± 285	109 ± 2
20.00	461 ± 0.5	22 ± 2	192,533 ± 13,954	86 ± 1	0.5568 ± 0.0012	77,480 ± 283	77,414 ± 283	107 ± 2
23.75	433 ± 0.4	10 ± 1	396,030 ± 45,084	87 ± 1	0.5571 ± 0.0008	77,443 ± 210	77,380 ± 210	108 ± 2
25.00	453 ± 0.6	24 ± 1	171,066 ± 9,163	87 ± 2	0.5571 ± 0.0014	77,457 ± 330	77,391 ± 330	108 ± 2
29.00	316 ± 0.3	42 ± 2	69,414 ± 3,290	91 ± 2	0.5602 ± 0.0014	77,605 ± 335	77,537 ± 335	113 ± 2
39.75	384 ± 0.3	31 ± 1	117,230 ± 5,263	96 ± 1	0.5654 ± 0.0008	78,082 ± 224	78,018 ± 224	119 ± 2
58.00	209 ± 0.3	194 ± 4	10,101 ± 223	97 ± 2	0.5683 ± 0.0025	78,543 ± 536	78,456 ± 537	121 ± 2
70.75	463 ± 0.5	53 ± 2	82,524 ± 2,504	109 ± 1	0.5780 ± 0.0008	79,125 ± 230	79,060 ± 230	136 ± 2
147.00	211 ± 0.3	30 ± 2	68,306 ± 3,955	120 ± 2	0.5937 ± 0.0019	80,959 ± 417	80,892 ± 417	151 ± 2
168.50	370 ± 0.3	76 ± 2	48,569 ± 1,244	134 ± 1	0.6024 ± 0.0009	81,108 ± 234	81,041 ± 234	168 ± 2

Sample (mm dft)	$^{238}\text{U}$ [ng g <sup>-1</sup> ]	$^{232}\text{Th}$ [pg g <sup>-1</sup> ]	$^{230}\text{Th} / ^{232}\text{Th}$ (atomic x10 <sup>-6</sup> )	$\delta^{234}\text{U}^*$ (measured)	$^{230}\text{Th} / ^{238}\text{U}^\dagger$ (activity)	Uncorrected Age (a)§	Corrected Age (a)#	$\delta^{234}\text{U}^*$ (initial)
<b><u>GAS12</u></b>								
190.00	192 ± 0.2	54 ± 2	35,131 ± 1,279	120 ± 2	0.5992 ± 0.0019	81,999 ± 426	81,929 ± 426	152 ± 2
<b><u>GAS13</u></b>								
7.25	118 ± 0.1	143 ± 3	7,280 ± 170	52 ± 1	0.5344 ± 0.0024	76,815 ± 523	76,719 ± 523	64 ± 2
11.00	247 ± 0.2	88 ± 2	24,815 ± 682	51 ± 1	0.5350 ± 0.0011	77,028 ± 280	76,954 ± 280	63 ± 2
15.00	383 ± 0.5	42 ± 1	79,942 ± 1,932	46 ± 2	0.5329 ± 0.0011	77,202 ± 288	77,138 ± 288	57 ± 2
23.00	418 ± 0.4	57 ± 2	64,474 ± 1,851	45 ± 1	0.5340 ± 0.0009	77,469 ± 250	77,401 ± 250	56 ± 2
31.75	419 ± 0.4	96 ± 3	38,304 ± 1,098	46 ± 1	0.5343 ± 0.0008	77,446 ± 230	77,376 ± 230	57 ± 2
52.00	442 ± 0.4	28 ± 2	141,138 ± 7,662	47 ± 1	0.5369 ± 0.0009	77,851 ± 241	77,785 ± 241	59 ± 2
78.75	373 ± 0.3	96 ± 3	34,570 ± 911	51 ± 1	0.5409 ± 0.0008	78,248 ± 238	78,178 ± 238	64 ± 2
85.00	232 ± 0.2	20 ± 2	104,163 ± 10,256	49 ± 1	0.5405 ± 0.0015	78,433 ± 354	78,367 ± 354	61 ± 2
95.75	409 ± 0.4	239 ± 5	15,285 ± 323	50 ± 1	0.5414 ± 0.0008	78,494 ± 239	78,415 ± 240	62 ± 2
111.00	490 ± 0.6	44 ± 2	99,706 ± 5,094	49 ± 2	0.5406 ± 0.0011	78,484 ± 292	78,417 ± 292	61 ± 2
120.00	442 ± 0.4	37 ± 2	105,776 ± 5,544	49 ± 1	0.5426 ± 0.0009	78,856 ± 259	78,790 ± 259	61 ± 2
134.75	456 ± 0.5	18 ± 2	227,539 ± 24,237	50 ± 2	0.5449 ± 0.0011	79,231 ± 294	79,168 ± 294	62 ± 2
171.00	488 ± 0.5	333 ± 7	13,320 ± 269	50 ± 1	0.5506 ± 0.0009	80,380 ± 265	80,300 ± 266	63 ± 2
<b><u>GAS22</u></b>								
1.4	322 ± 0.3	150 ± 4	24,772 ± 591	108 ± 1	0.6975 ± 0.0011	105,810 ± 378	105,731 ± 378	146 ± 2
4.2	297 ± 1.3	62 ± 0.4	54,315 ± 290	103 ± 1	0.6921 ± 0.0009	105,371 ± 355	105,299 ± 355	139 ± 2
7.4	305 ± 1	17 ± 0.1	205,514 ± 1,212	103 ± 2	0.6916 ± 0.0009	105,227 ± 376	105,159 ± 376	139 ± 2
9.8	337 ± 0.4	16 ± 1	242,747 ± 14,749	102 ± 1	0.6915 ± 0.0011	105,313 ± 378	105,244 ± 378	138 ± 2
12.2	317 ± 2	16 ± 0.1	221,352 ± 1,371	104 ± 2	0.6911 ± 0.0011	104,932 ± 404	104,864 ± 404	140 ± 2
17.4	325 ± 0.4	19 ± 1	195,158 ± 10,918	102 ± 2	0.6945 ± 0.0010	106,247 ± 369	106,178 ± 369	137 ± 2
20.4	262 ± 1	19 ± 0.1	158,654 ± 943	100 ± 2	0.6927 ± 0.0010	105,998 ± 378	105,929 ± 378	135 ± 2
24.8	311 ± 1	13 ± 0.1	274,463 ± 1,776	99 ± 2	0.6922 ± 0.0010	106,056 ± 380	105,988 ± 380	134 ± 2
28.8	340 ± 0.3	39 ± 1	99,845 ± 3,321	100 ± 1	0.6933 ± 0.0009	106,145 ± 324	106,075 ± 324	135 ± 2
41.1	353 ± 0.5	10 ± 1	419,777 ± 60,479	101 ± 2	0.6954 ± 0.0018	106,636 ± 575	106,573 ± 575	136 ± 3
49.8	172 ± 0.2	13 ± 2	155,310 ± 20,730	102 ± 2	0.6963 ± 0.0023	106,552 ± 673	106,487 ± 673	138 ± 2
55.8	321 ± 0.3	29 ± 4	125,513 ± 16,346	100 ± 1	0.6985 ± 0.0014	107,556 ± 430	107,487 ± 430	135 ± 2
62.8	347 ± 0.4	89 ± 3	44,715 ± 1,450	99 ± 1	0.6946 ± 0.0011	106,677 ± 380	106,603 ± 380	134 ± 2
67.4	352 ± 0.3	26 ± 2	157,626 ± 9,298	100 ± 1	0.6974 ± 0.0011	107,352 ± 380	107,286 ± 381	135 ± 2
81.8	339 ± 0.3	12 ± 2	328,531 ± 56,430	96 ± 1	0.6954 ± 0.0012	107,565 ± 368	107,497 ± 368	129 ± 2
99.8	309 ± 0.3	61 ± 2	58,409 ± 1,656	106 ± 1	0.7038 ± 0.0010	107,827 ± 355	107,758 ± 355	144 ± 2
<b><u>GAS25</u></b>								
58.50	295 ± 0.3	455 ± 9	6132 ± 125	61 ± 2	0.5737 ± 0.0011	84,045 ± 339	83,942 ± 340	77 ± 2

Sample (mm dft)	$^{238}\text{U}$ [ng g <sup>-1</sup> ]	$^{232}\text{Th}$ [pg g <sup>-1</sup> ]	$^{230}\text{Th} / ^{232}\text{Th}$ (atomic x10 <sup>-6</sup> )	$\delta^{234}\text{U}^*$ (measured)	$^{230}\text{Th} / ^{238}\text{U}^\dagger$ (activity)	Uncorrected Age (a)§	Corrected Age (a)#	$\delta^{234}\text{U}^*$ (initial)
<b><u>GAS25</u></b>								
66.00	401 ± 0.4	27 ± 2	141,308 ± 7,990	61 ± 1	0.5752 ± 0.0010	84,383 ± 284	84,317 ± 284	77 ± 2
76.25	315 ± 0.3	52 ± 2	58,083 ± 1,936	63 ± 1	0.5769 ± 0.0010	84,518 ± 285	84,450 ± 285	80 ± 2
78.50	315 ± 0.4	23 ± 1	129,751 ± 7,210	60 ± 2	0.5759 ± 0.0012	84,592 ± 356	84,528 ± 356	77 ± 2
79.75	299 ± 0.3	35 ± 2	81,909 ± 3,797	66 ± 2	0.5785 ± 0.0016	84,426 ± 427	84,359 ± 427	84 ± 2
81.00	276 ± 0.3	59 ± 2	45,241 ± 1,561	69 ± 1	0.5816 ± 0.0010	84,714 ± 296	84,644 ± 296	88 ± 2
84.75	249 ± 0.2	91 ± 2	26,228 ± 667	69 ± 2	0.5823 ± 0.0014	84,801 ± 380	84,728 ± 380	88 ± 2
Hiatus								
89.50	356 ± 0.4	73 ± 2	48,885 ± 1,451	84 ± 1	0.6063 ± 0.0011	88,126 ± 311	88,056 ± 311	108 ± 2
95.75	326 ± 0.3	42 ± 2	77,356 ± 2,847	85 ± 1	0.6083 ± 0.0011	88,437 ± 303	88,371 ± 303	109 ± 2
99.50	430 ± 0.4	10 ± 1	420,386 ± 51,620	85 ± 1	0.6096 ± 0.0010	88,679 ± 286	88,614 ± 286	109 ± 2
104.00	386 ± 0.3	587 ± 12	6,623 ± 135	87 ± 1	0.6109 ± 0.0009	88,722 ± 262	88,615 ± 262	112 ± 2
110.00	363 ± 0.3	93 ± 2	39,258 ± 1,006	86 ± 1	0.6111 ± 0.0008	88,899 ± 267	88,825 ± 267	111 ± 2
117.00	426 ± 0.4	29 ± 2	146,933 ± 7,574	90 ± 2	0.6144 ± 0.0008	89,064 ± 277	88,995 ± 277	116 ± 2
123.75	414 ± 0.4	48 ± 2	86,637 ± 4,324	87 ± 1	0.6138 ± 0.0009	89,403 ± 268	89,333 ± 268	112 ± 2
155.75	436 ± 0.6	106 ± 3	42,484 ± 1,049	103 ± 2	0.6290 ± 0.0012	90,455 ± 385	90,386 ± 385	134 ± 3
180.75	412 ± 0.4	56 ± 2	76,195 ± 2,723	93 ± 1	0.6235 ± 0.0011	90,742 ± 322	90,672 ± 322	120 ± 2
204.50	425 ± 0.5	77 ± 2	56,793 ± 1,443	93 ± 2	0.6246 ± 0.0012	90,922 ± 363	90,856 ± 363	120 ± 2
<b><u>GAS27</u></b>								
152.75	255 ± 0.3	49 ± 2	60,104 ± 2,379	135 ± 1	0.7053 ± 0.0012	103,176 ± 364	103,105 ± 364	180 ± 2
162.75	583 ± 0.7	25 ± 2	269,724 ± 18,755	132 ± 2	0.7054 ± 0.0010	103,586 ± 342	103,518 ± 342	177 ± 2
169.00	344 ± 0.4	9 ± 1	420,035 ± 46,871	128 ± 2	0.7025 ± 0.0010	103,655 ± 345	103,587 ± 345	171 ± 2
174.50	346 ± 0.3	13 ± 2	300,677 ± 35,248	123 ± 1	0.7004 ± 0.0009	103,941 ± 329	103,873 ± 329	165 ± 2
181.50	351 ± 0.4	19 ± 2	209,908 ± 16,984	122 ± 2	0.7002 ± 0.0016	104,044 ± 498	103,980 ± 498	164 ± 2
184.50	359 ± 0.4	66 ± 2	62,558 ± 1,685	120 ± 2	0.6993 ± 0.0010	104,130 ± 370	104,058 ± 370	162 ± 2
188.25	377 ± 0.3	20 ± 1	219,403 ± 15,795	119 ± 1	0.7003 ± 0.0010	104,542 ± 339	104,473 ± 339	160 ± 2
196.00	328 ± 0.4	7 ± 1	559,710 ± 85,363	116 ± 2	0.6980 ± 0.0010	104,623 ± 361	104,555 ± 361	155 ± 2
209.75	327 ± 0.3	79 ± 2	47,623 ± 1,481	109 ± 2	0.6938 ± 0.0014	104,788 ± 437	104,715 ± 437	146 ± 2
<b><u>GAS29</u></b>								
51.25	330 ± 0.3	291 ± 6	13,228 ± 276	129 ± 1	0.7077 ± 0.0010	104,658 ± 349	104,573 ± 350	174 ± 2
56.25	283 ± 1	32 ± 1	104,411 ± 571	125 ± 1	0.7053 ± 0.0010	104,810 ± 332	104,740 ± 332	168 ± 2
62.50	332 ± 0.3	16 ± 1	236,755 ± 21,567	129 ± 1	0.7100 ± 0.0011	105,271 ± 354	105,207 ± 354	174 ± 2
78.75	346 ± 0.4	147 ± 3	27,358 ± 617	122 ± 2	0.7064 ± 0.0010	105,549 ± 368	105,475 ± 368	165 ± 2
97.50	348 ± 0.4	118 ± 3	34,306 ± 847	118 ± 1	0.7053 ± 0.0014	106,026 ± 416	105,954 ± 416	159 ± 2
113.75	273 ± 0.3	133 ± 3	23,937 ± 540	117 ± 1	0.7073 ± 0.0012	106,717 ± 380	106,642 ± 380	158 ± 2



**Table S1: MC-ICP-MS U-Th dating results of samples analysed in this study.**

**mm dft = distance from top in mm.**

**All uncertainties are  $2\sigma$ .**

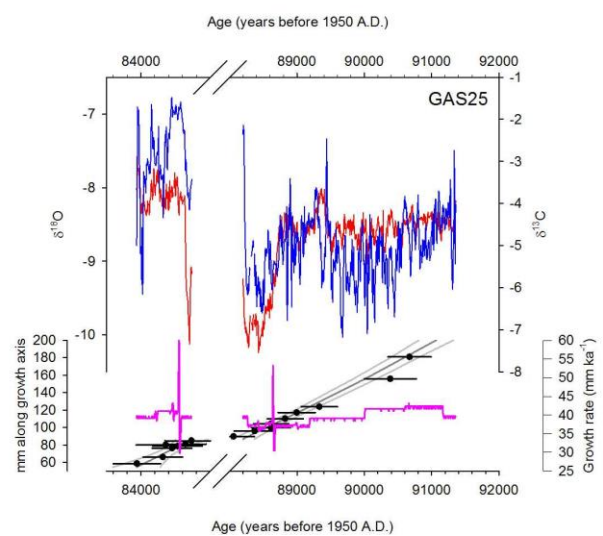
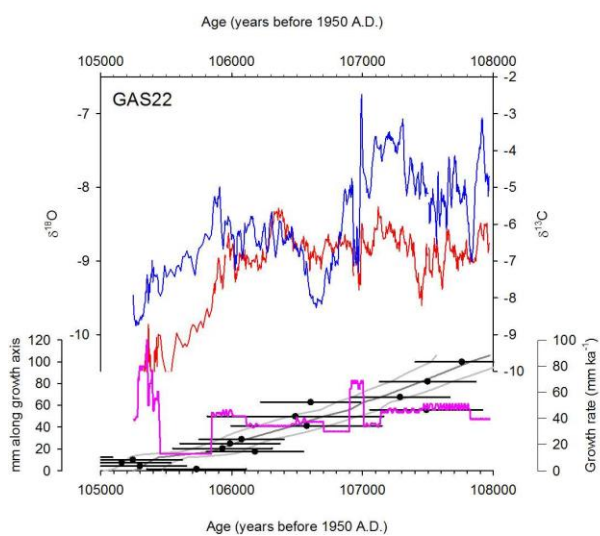
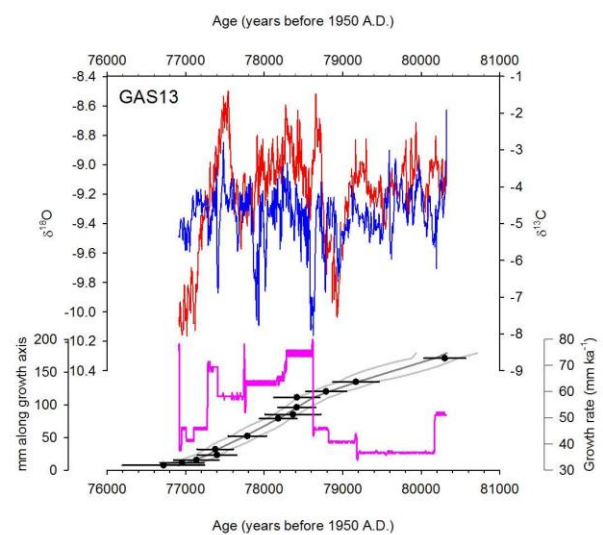
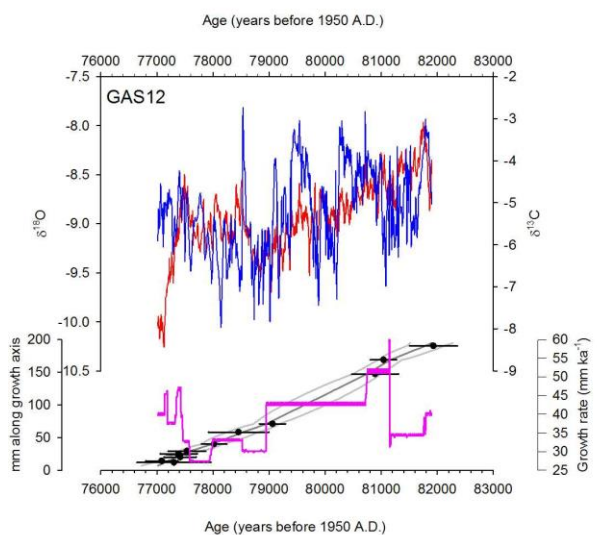
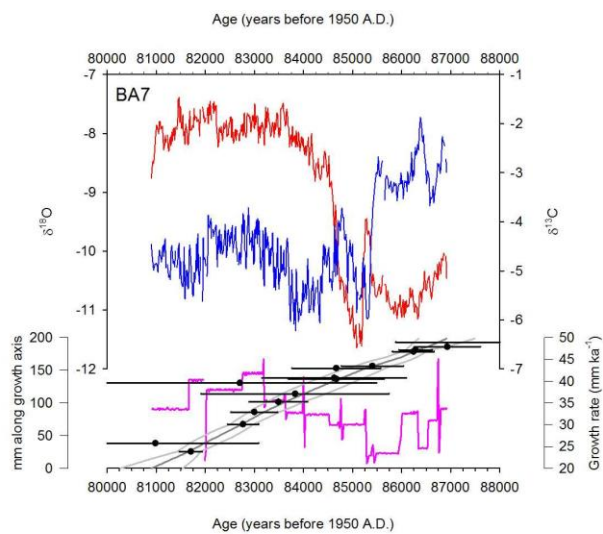
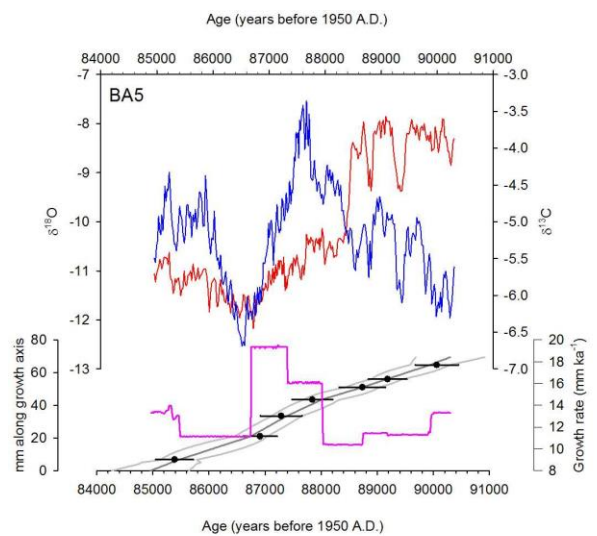
**\*  $\delta^{234}\text{U} = ([^{234}\text{U}/^{238}\text{U}]_{\text{activity}} - 1) \times 1000$ .**

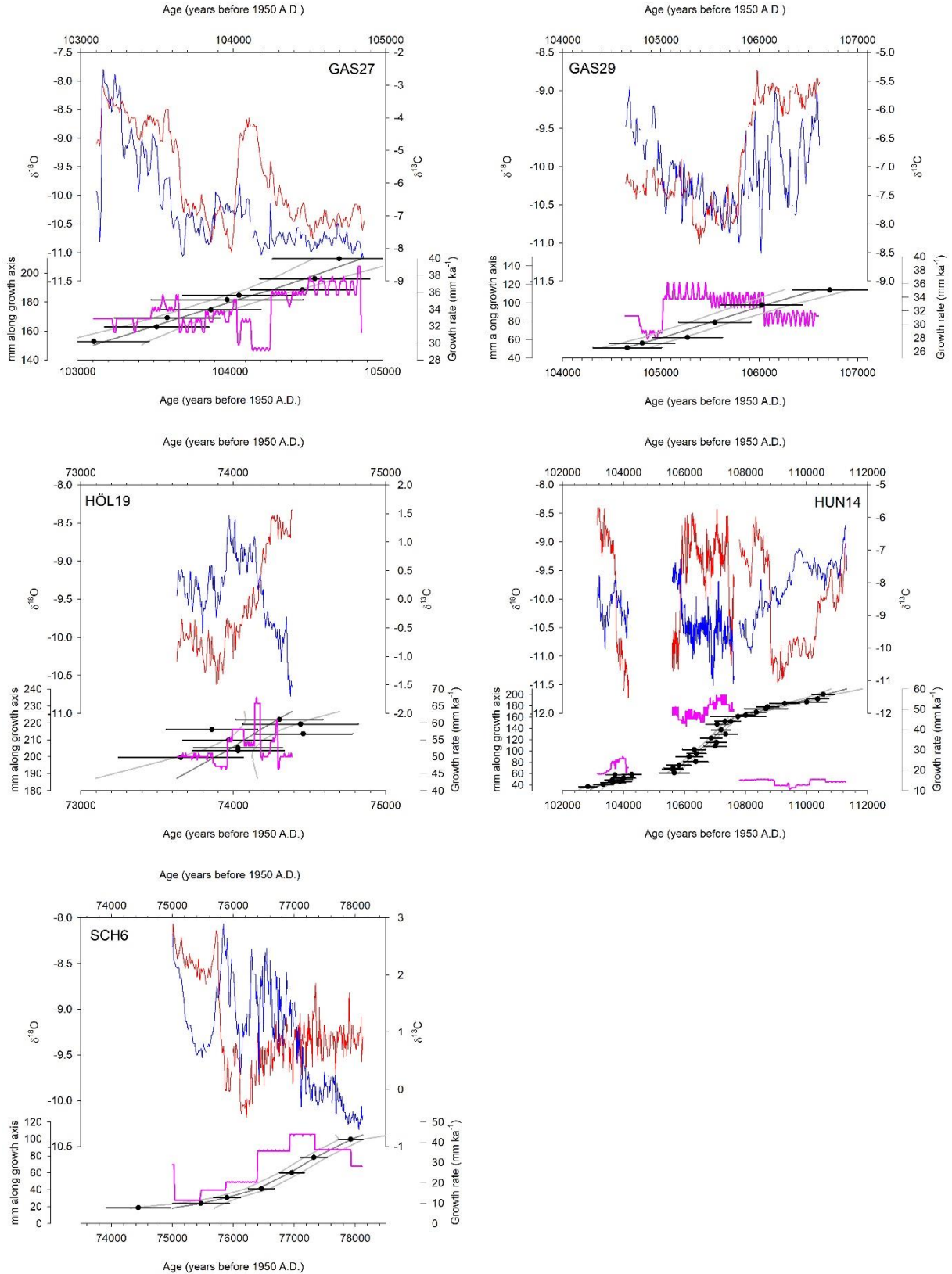
**†  $[^{230}\text{Th}/^{238}\text{U}]_{\text{activity}} = 1 - e^{-\lambda_{230}T} + (\delta^{234}\text{U}_{\text{measured}}/1000)[\lambda_{230}/(\lambda_{230} - \lambda_{234})](1 - e^{-(\lambda_{230} - \lambda_{234})T})$ , where T is age in years.  $\lambda_{230} = 9.1705 \times 10^{-6} \text{ a}^{-1}$  (Cheng et al., 2013),**

**$\lambda_{234} = 2.8221 \times 10^{-6} \text{ a}^{-1}$  (Cheng et al., 2013),  $\lambda_{238} = 1.551 \times 10^{-1} \text{ a}^{-1}$  (Jaffey et al., 1971).**

**§ Years before measurement and without detrital Th correction.**

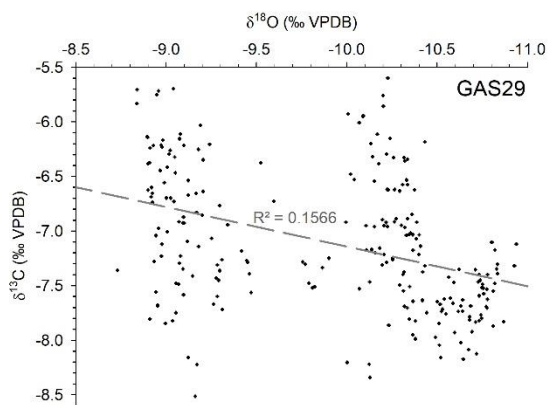
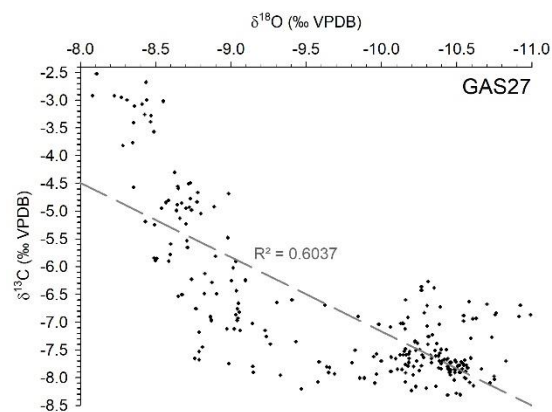
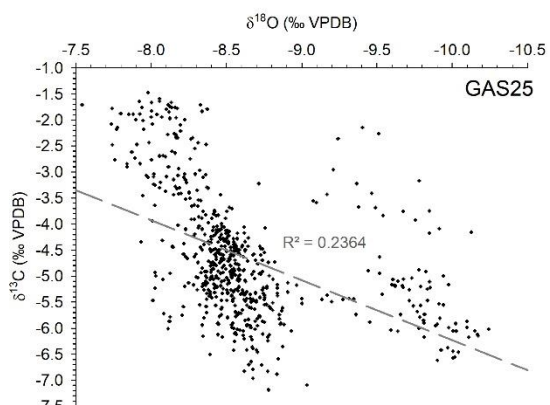
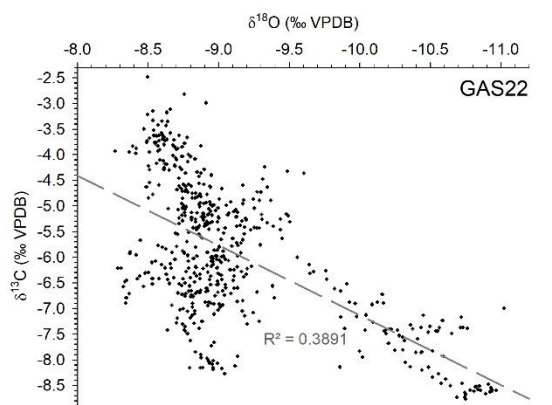
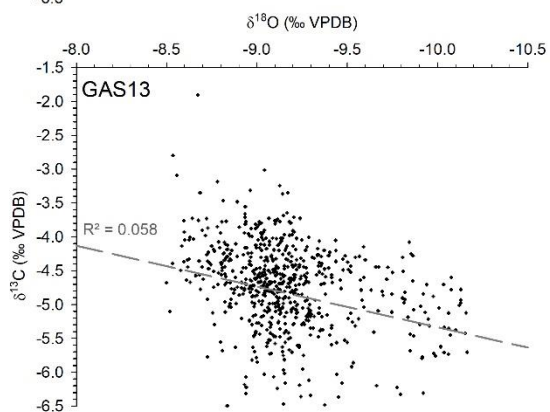
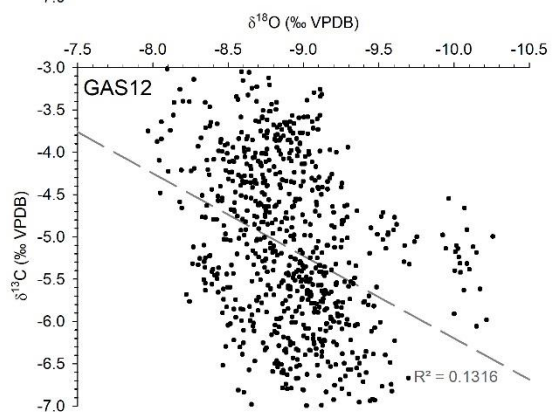
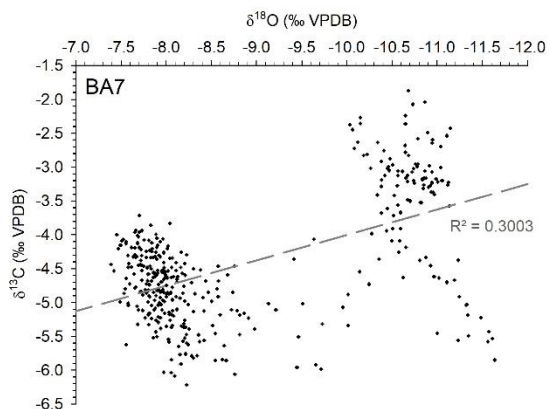
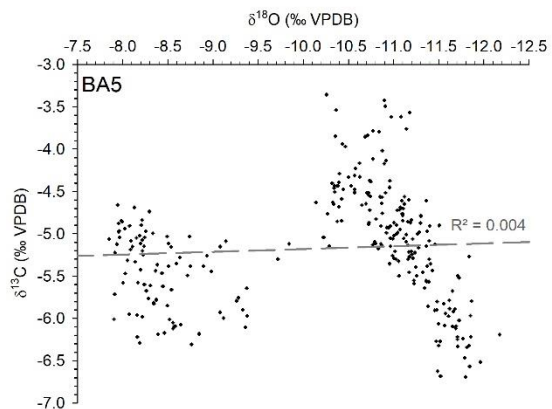
**# Years before 1950 A.D.. Most samples corrected for detrital Th contamination using the bulk earth atomic value of  $4.4 \pm 2.2$  ppm for initial  $^{230}\text{Th}/^{232}\text{Th}_{\text{act}}$  (Wedepohl, 1995). Höl-19 is corrected using an isochron derived value of  $2.28 \times 10^{-6} \pm 0.86 \times 10^{-6}$ , which is inline with previous estimates from this cave (Moseley et al., 2014). The degree of detrital  $^{230}\text{Th}$  contamination is indicated by the measured ( $^{230}\text{Th}/^{232}\text{Th}$ ) activity ratio.**

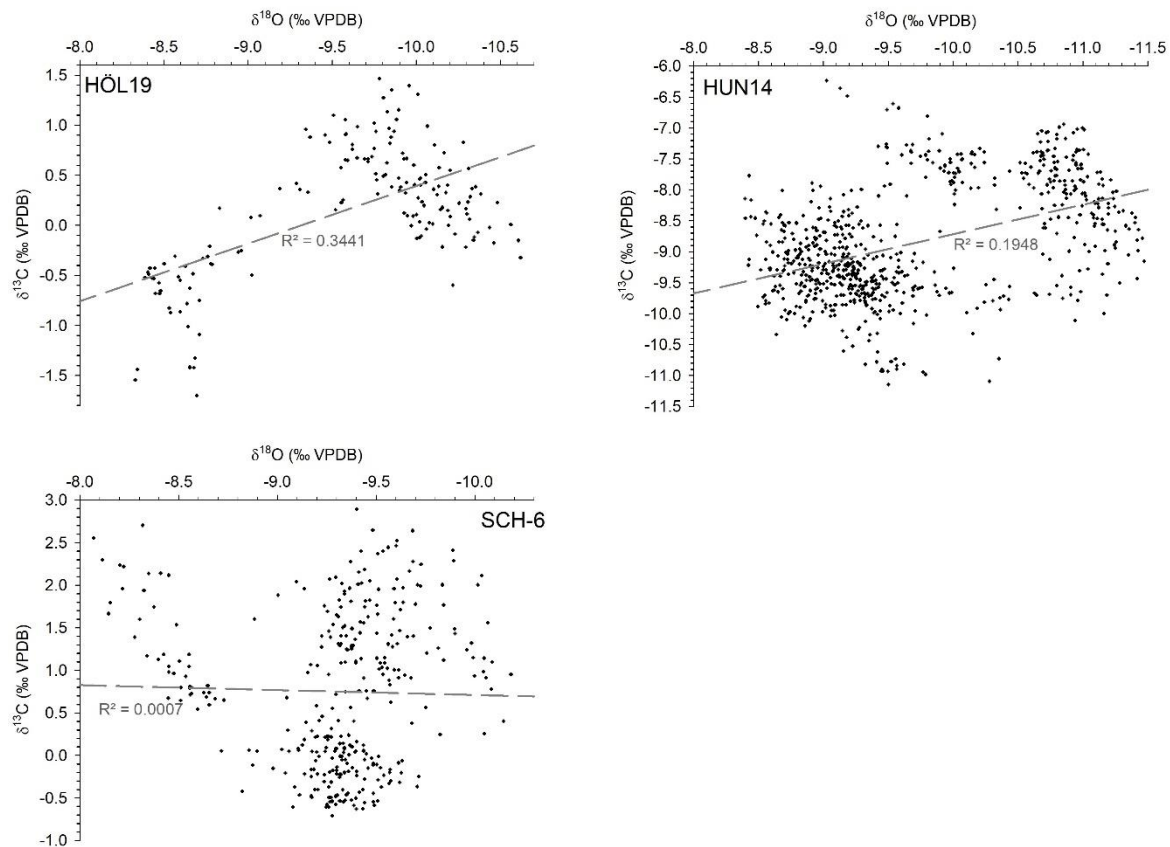




**Figure S3: Age modelling results for samples analysed in this study. Upper graphs show  $\delta^{18}\text{O}$  (red) and  $\delta^{13}\text{C}$  (blue) plotted on the Oxcal age model. Lower graphs show the U-Th ages with 2 sigma uncertainty used in the Oxcal age model (black circles with horizontal lines) plotted relative to distance along the growth axis. The dark grey line marks the central age model and the light grey lines mark the 2 sigma uncertainty. Pink lines show the growth rate.**



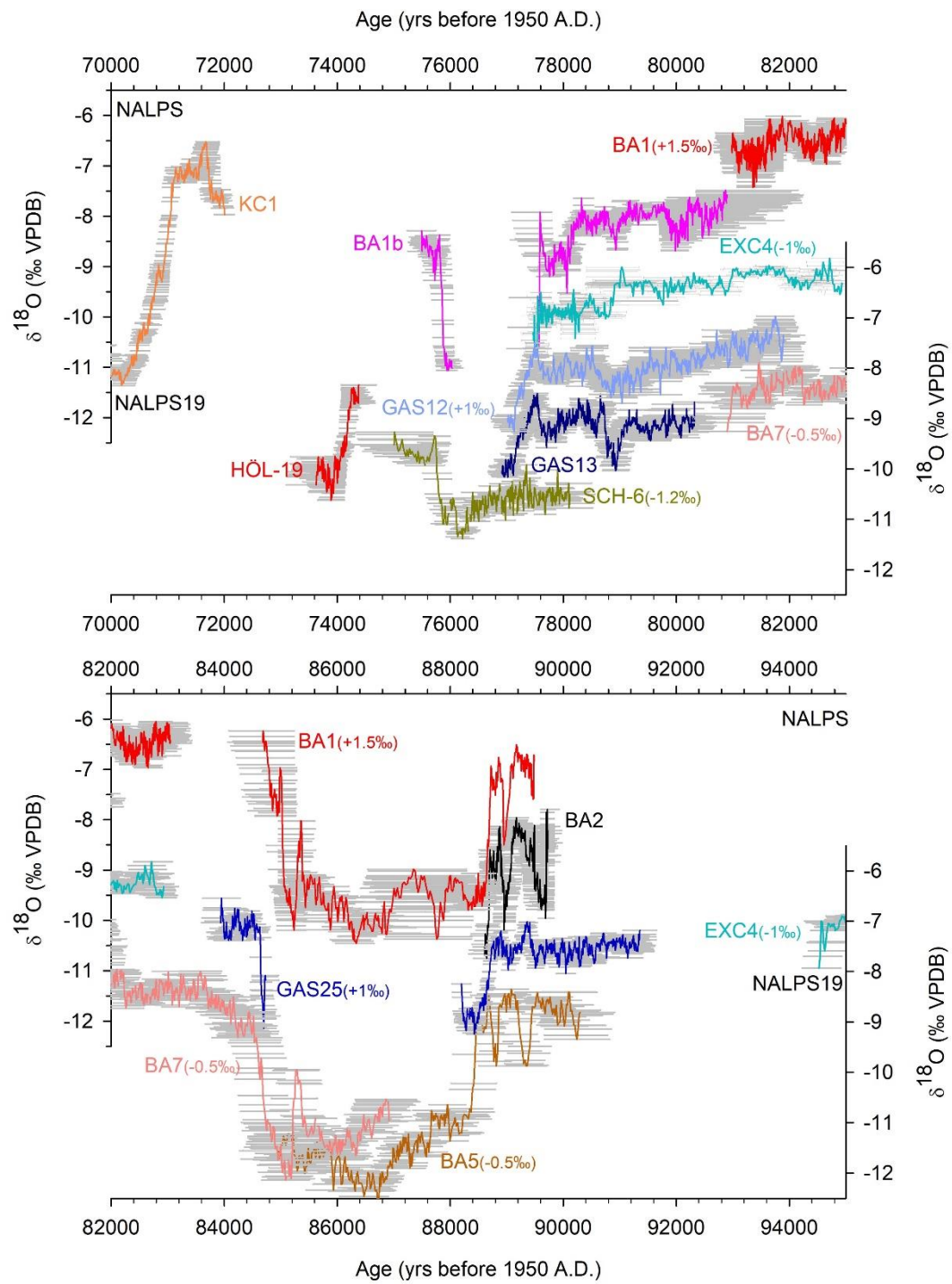




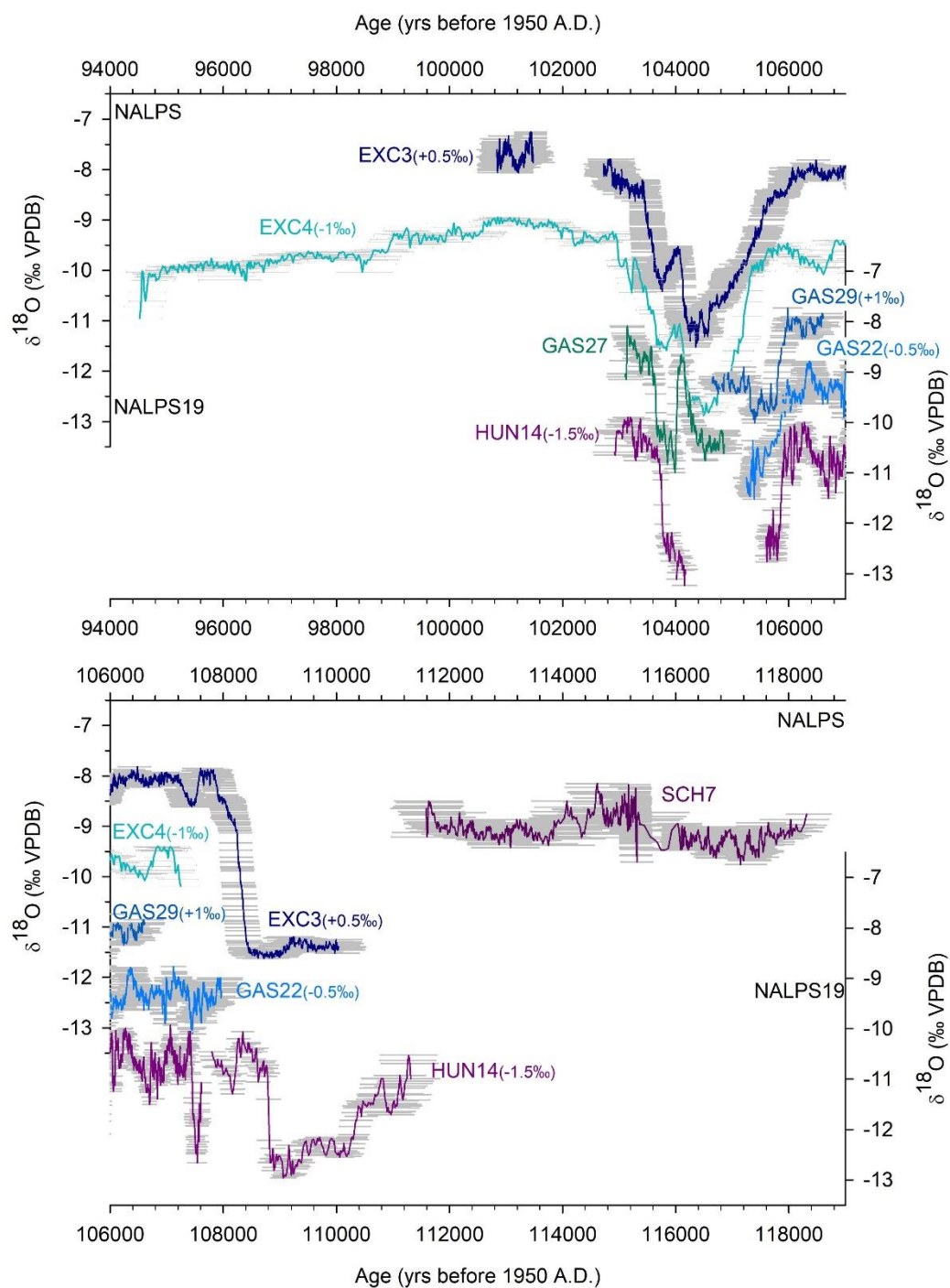
**Figure S4:**  $\delta^{18}\text{O}$  versus  $\delta^{13}\text{C}$  for each sample analysed in this study as well as the correlation coefficient ( $R^2$ ).

Sample	H1		H2		H3		H4		H5		H6	
	$\delta^{13}\text{C}$	$\delta^{18}\text{O}$	$\delta^{13}\text{C}$	$\delta^{18}\text{O}$	$\delta^{13}\text{C}$	$\delta^{18}\text{O}$	$\delta^{13}\text{C}$	$\delta^{18}\text{O}$	$\delta^{13}\text{C}$	$\delta^{18}\text{O}$	$\delta^{13}\text{C}$	$\delta^{18}\text{O}$
BA5	0.2	0.2	0.3	0.4								
BA7	0.5	0.3	0.4	0.3	0.3	0.3	0.4	0.4				
SCH6	0.9	0.4	0.3	0.7	1.0	0.6	0.4	0.2	0.5	0.3	0.3	0.3
HÖL19	0.4	0.3										
HUN14	0.9	0.2	0.6	0.4	0.5	0.2	0.3	0.3				
GAS22	2.8	0.4	1.6	0.5	3.2	0.3	1.6	0.3	2.3	0.4		
GAS25	2.0	0.4	1.9	0.2	1.3	0.6	0.6	0.2	0.6	0.2	0.9	0.2
GAS27	2.6	0.4	4.6	0.8	1.1	0.3	2.3	0.5	0.3	0.4		
GAS29	3.0	0.3	1.7	0.7	1.1	0.5	1.0	0.3	0.7	0.2		

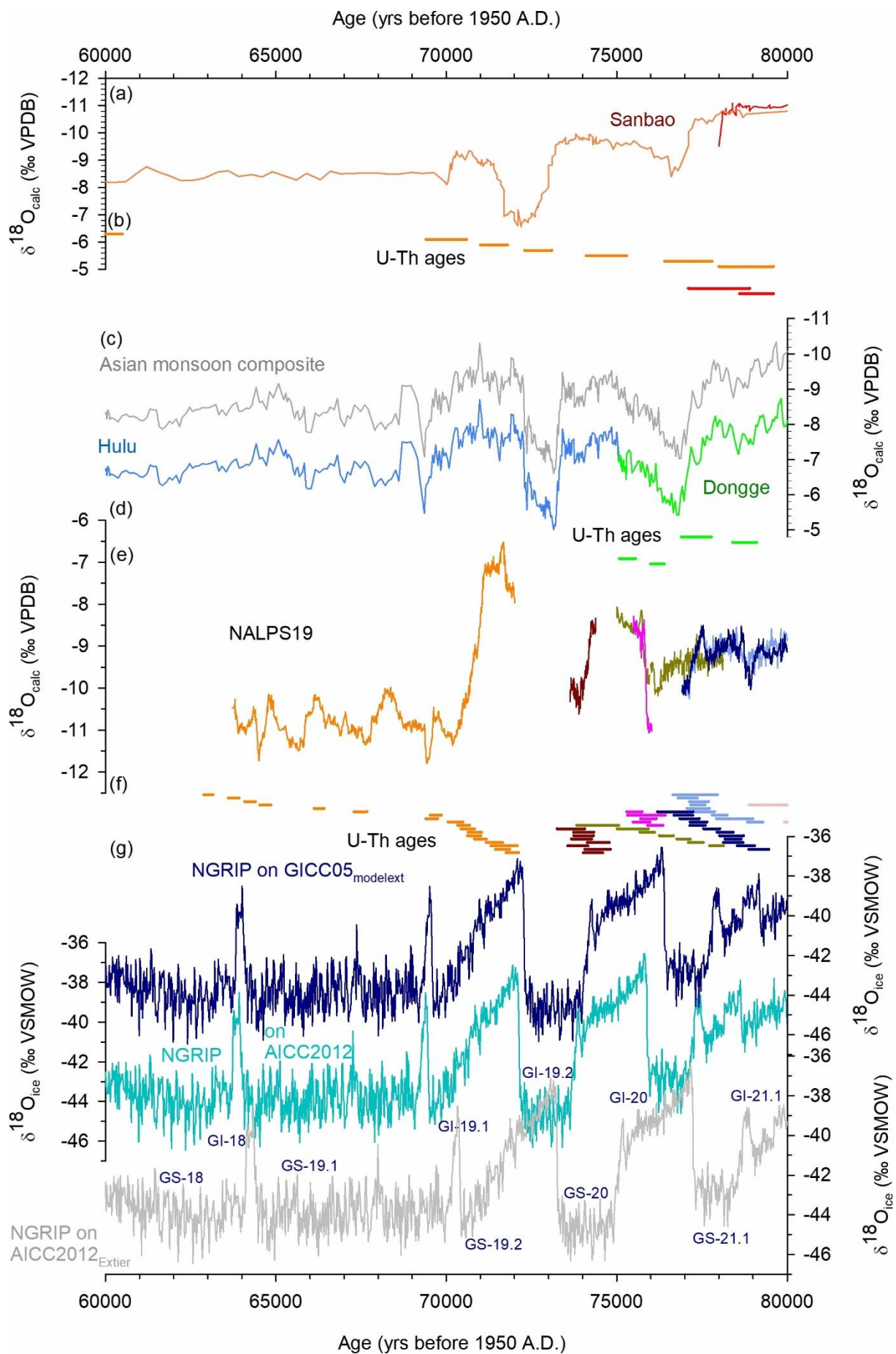
**Table S2:** Results of Hendy tests for the samples analysed in this study.

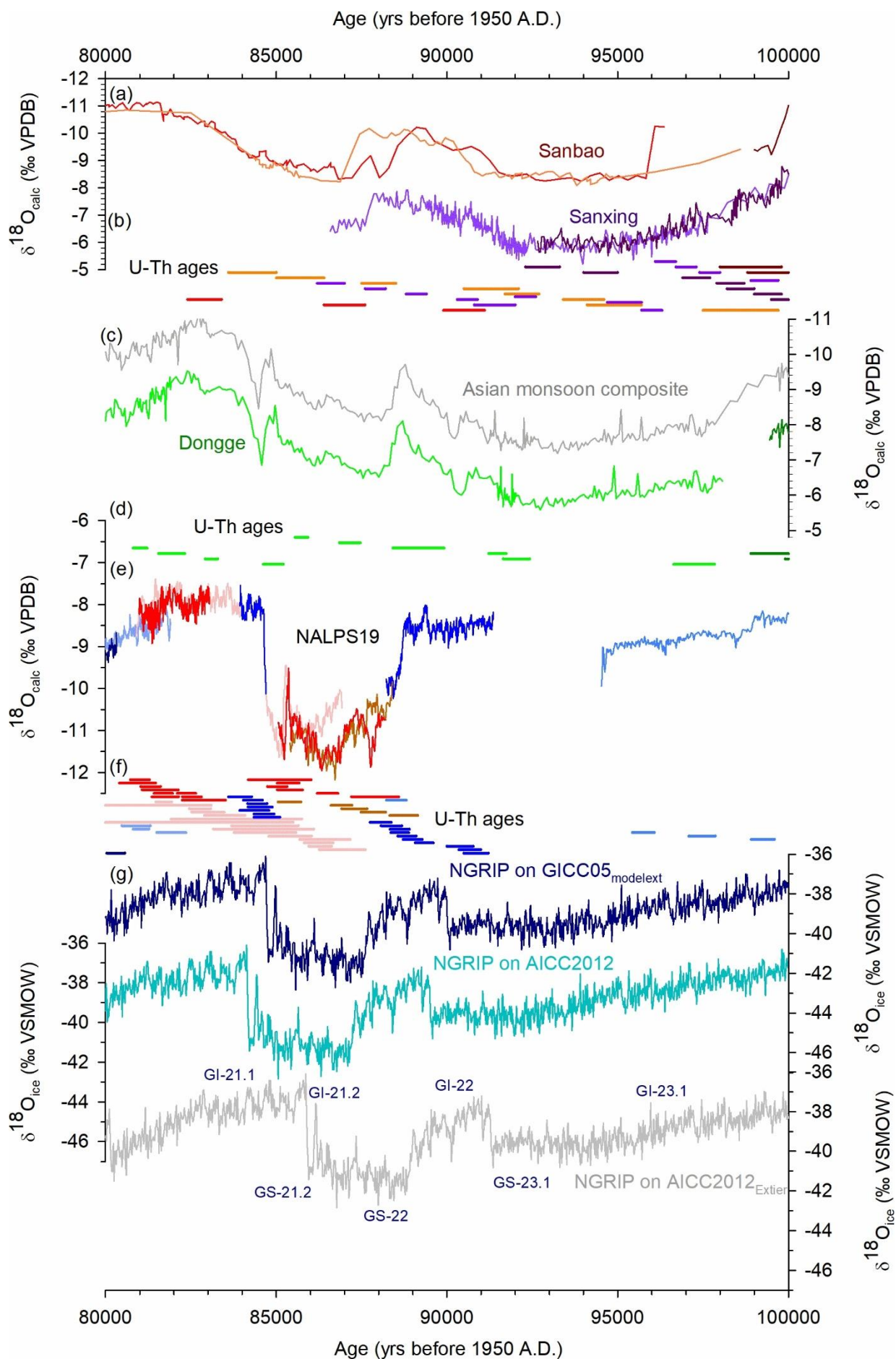




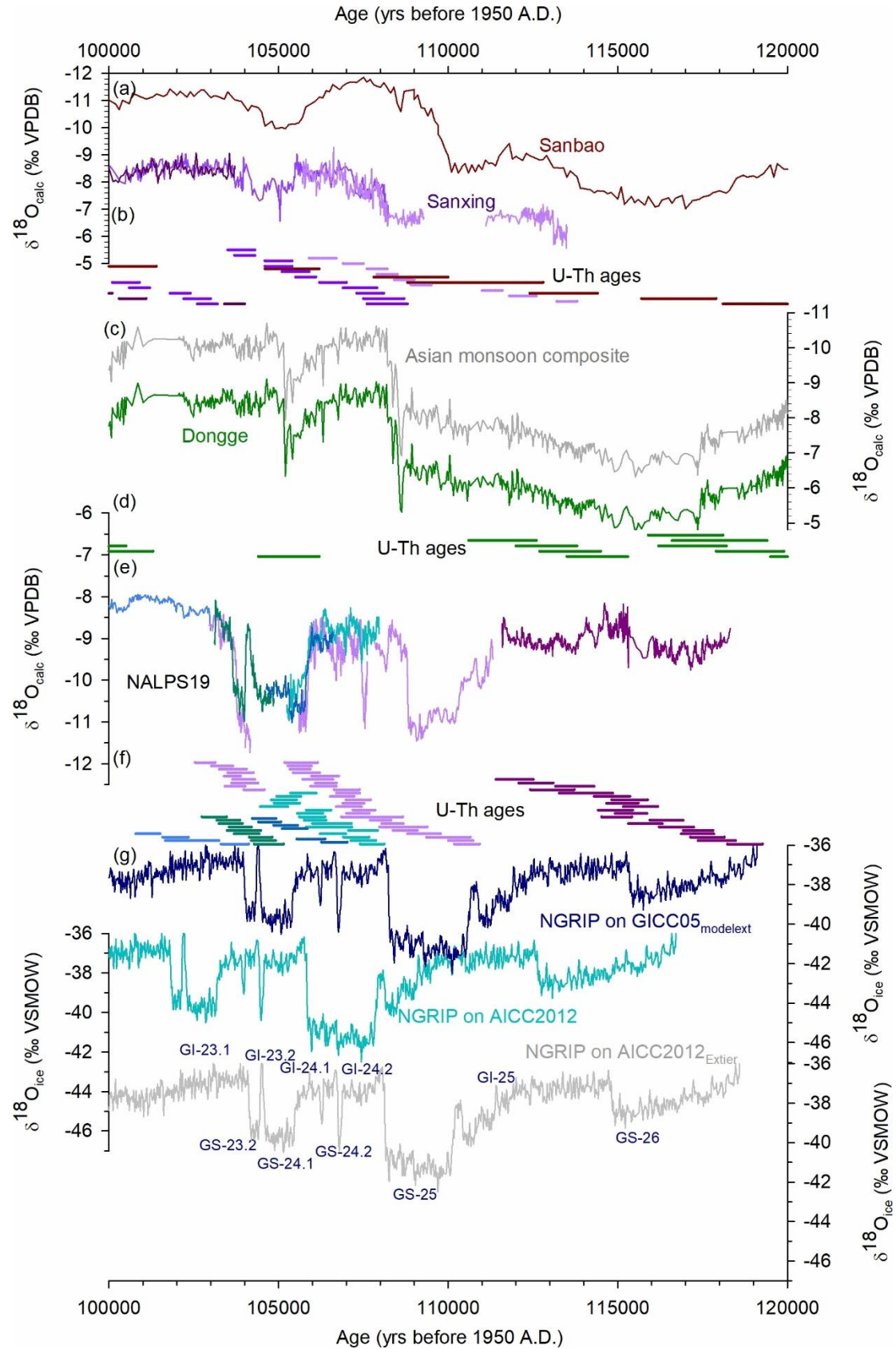


**Figure S5:**  $\delta^{18}\text{O}$  records of NALPS19 (this study) versus NALPS11 (Boch et al., 2011) including  $2\sigma$  uncertainty (grey horizontal bars). The records are shifted for ease of viewing; the direction and amount of shift are indicated in parentheses.



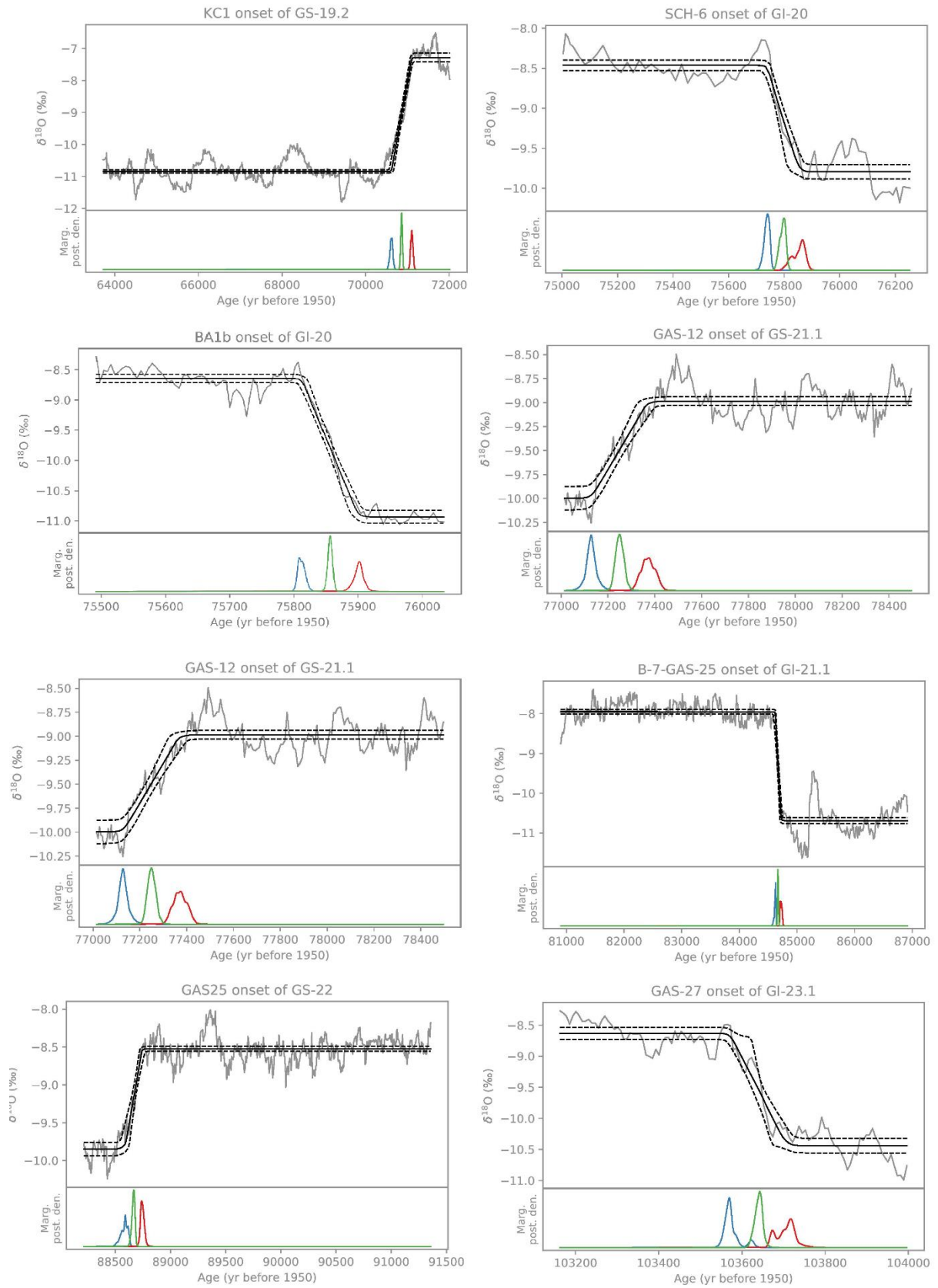






**Figure S6:** Fig. 3 from the main manuscript split into 20,000 year timeslices for ease of viewing. (a) Chinese speleothem  $\delta^{18}\text{O}$  records from Sanbao (Wang et al., 2008) and Sanxing (Jiang et al., 2016). (b)  $2\sigma$  range of U-Th ages for (a) colour-coded the same. (c) Asian monsoon composite record (Cheng et al., 2016) as well as the original data from which it is constructed (Dongge; Kelly et al., 2006; Kelly, 2010). (d)  $2\sigma$  range, of U-Th ages for (c) colour-coded the same. (e) NALPS19 record (this study). (f)  $2\sigma$  range of U-Th ages for (e) colour-coded the same. (g) NGRIP records on the GICC05<sub>modelext</sub> chronology (Svensson et al., 2008; Wolff et al., 2010), AICC2012 chronology (Veres et al., 2013), and AICC2012 revised according to Extier et al. (2018).





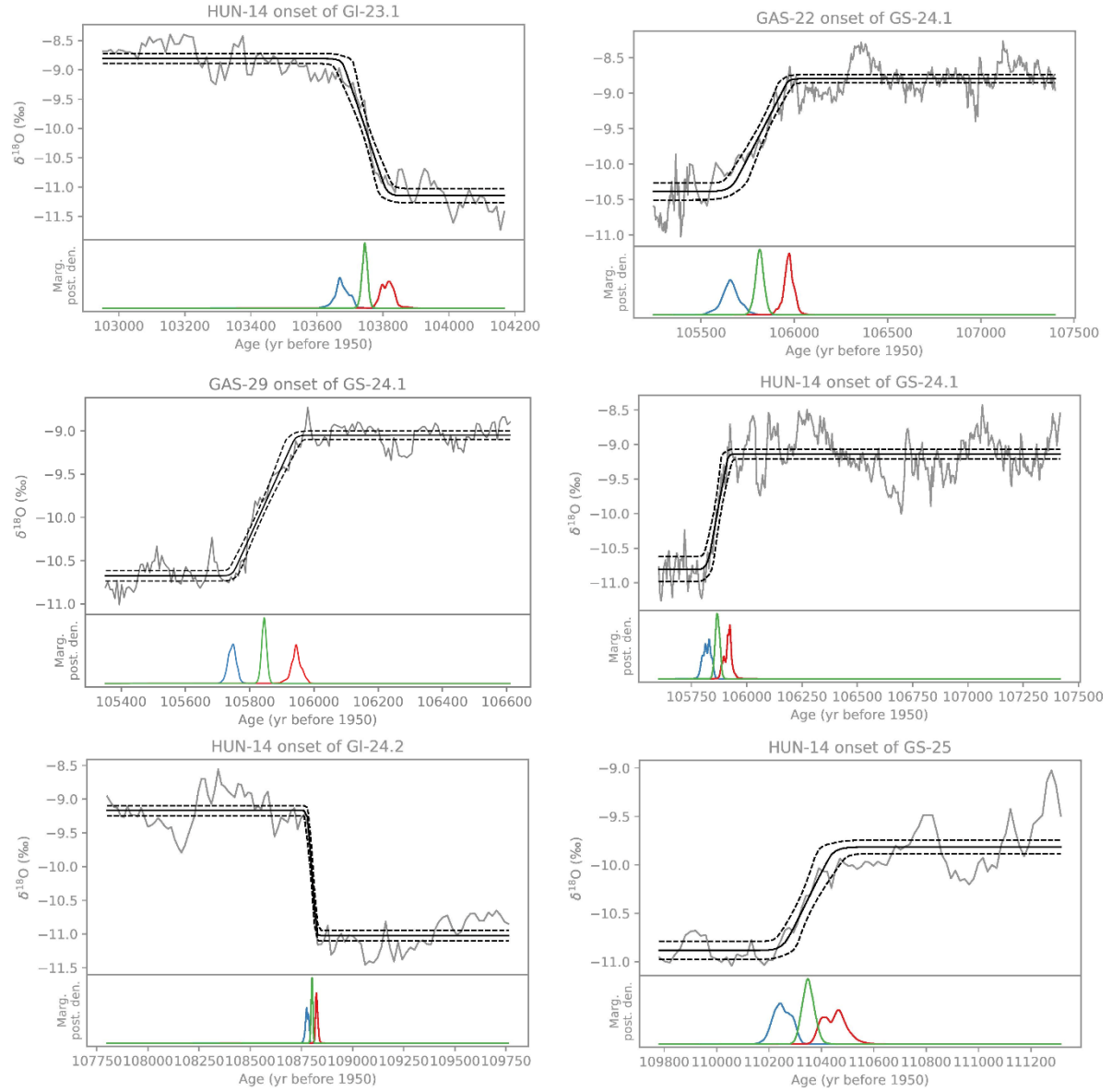


**Figure S7: Fitting results of the Erhardt et al. (2019) algorithm for the NALPS19 (chronology from this study). Each of the top panels shows the fitted data together with marginal posterior median and 5th and 95th percentile of the fitted ramp in solid and dashed lines respectively. The bottom panels show the marginal posterior densities for the onset, midpoint and endpoint of the transitions (in red, green and blue).**

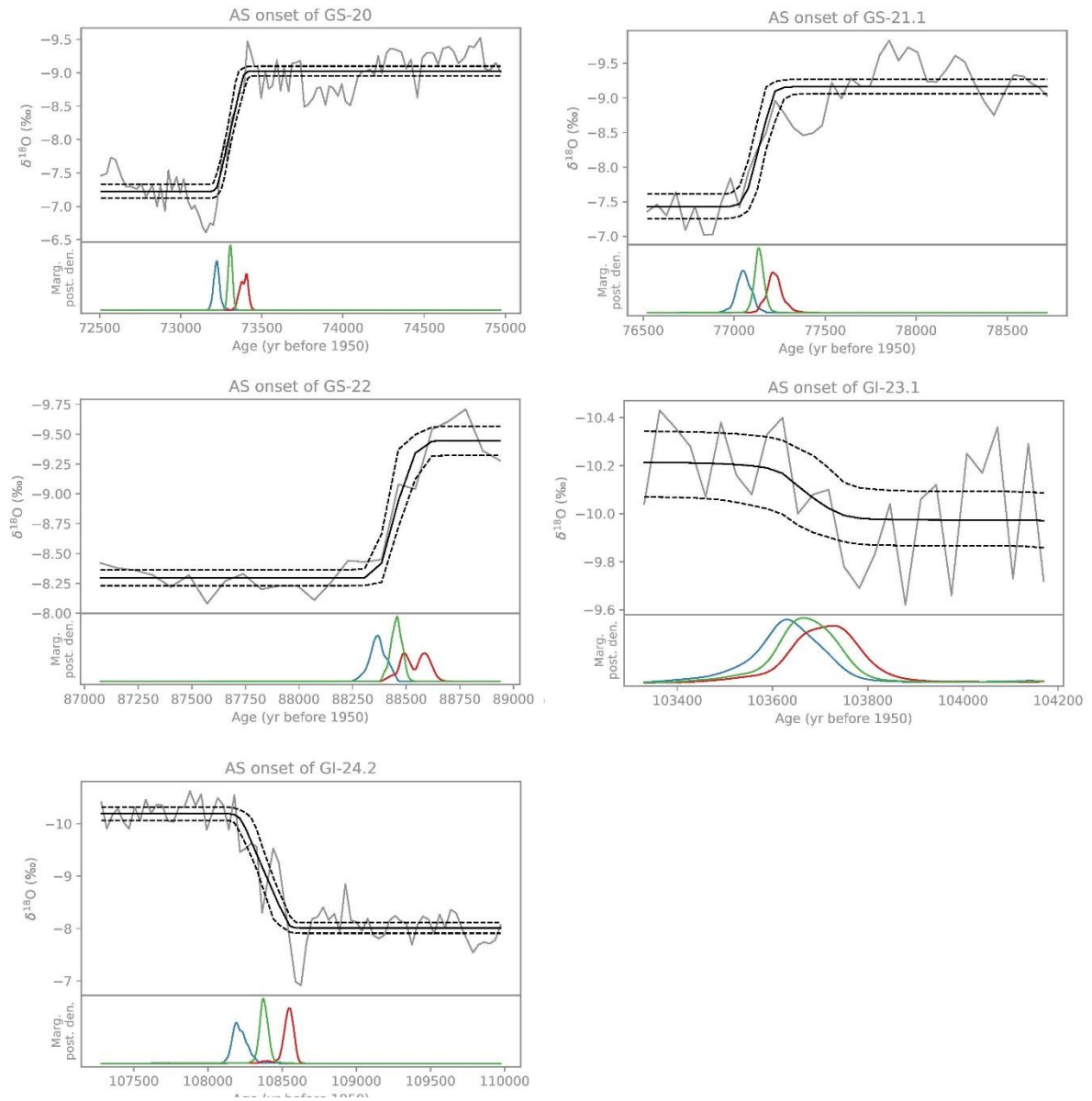


**Figure S7: Fitting results of the Erhardt et al. (2019) algorithm for the Asian monsoon composite (Kelly et al., 2006; Kelly, 2010; Cheng et al., 2016). Each of the top panels shows the fitted data together with marginal posterior median and 5th and 95th percentile of the fitted ramp in solid and dashed lines respectively. The bottom panels show the marginal posterior densities for the onset, midpoint and endpoint of the transitions (in red, green and blue).**

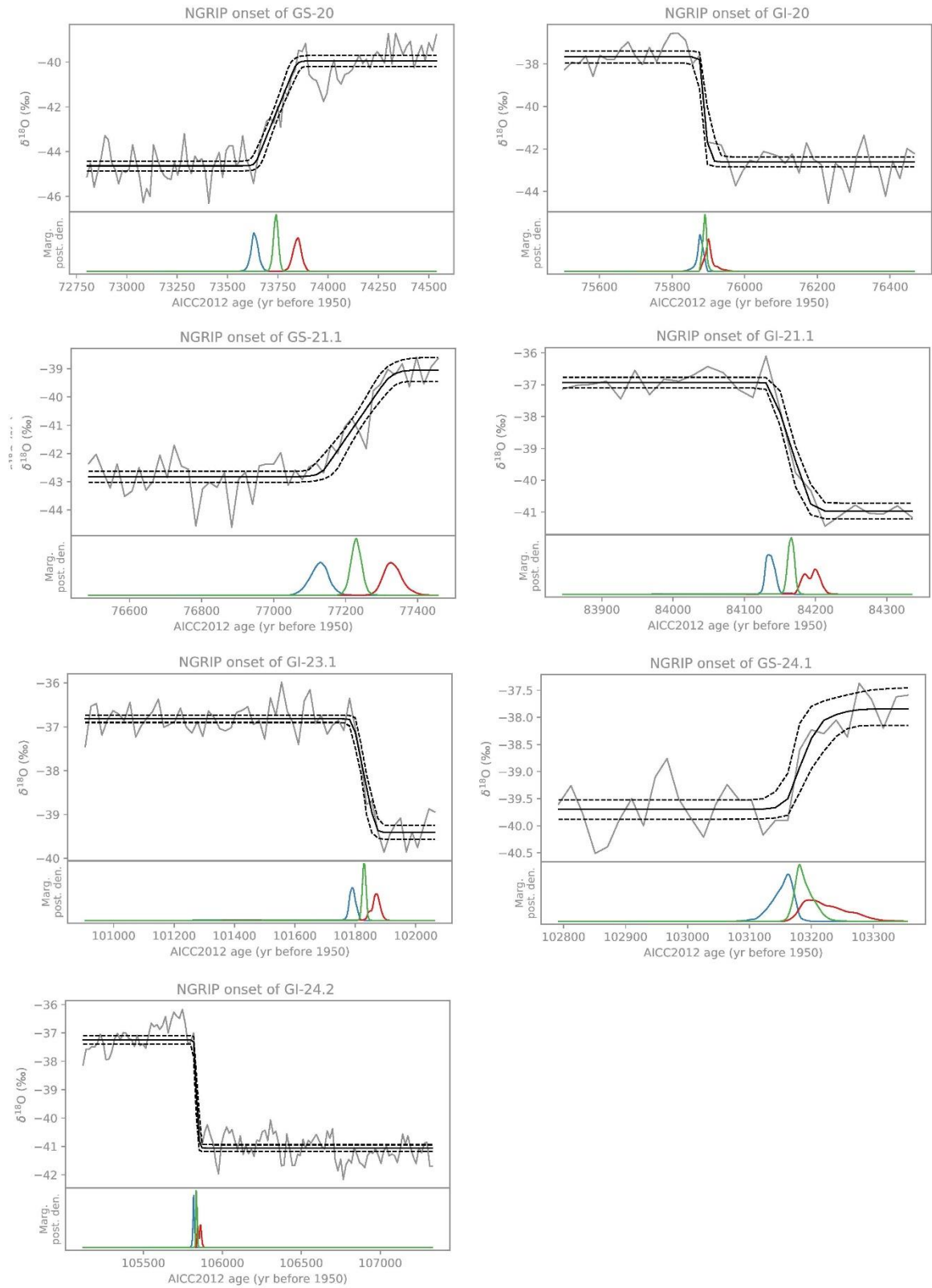


**Figure S7: Fitting results of the Erhardt et al. (2019) algorithm for NGRIP on the AICC2012 chronology (Veres et al., 2013). Each of the top panels shows the fitted data together with marginal posterior median and 5th and 95th percentile of the fitted ramp in solid and dashed lines respectively. The bottom panels show the marginal posterior densities for the onset, midpoint and endpoint of the transitions (in red, green and blue).**



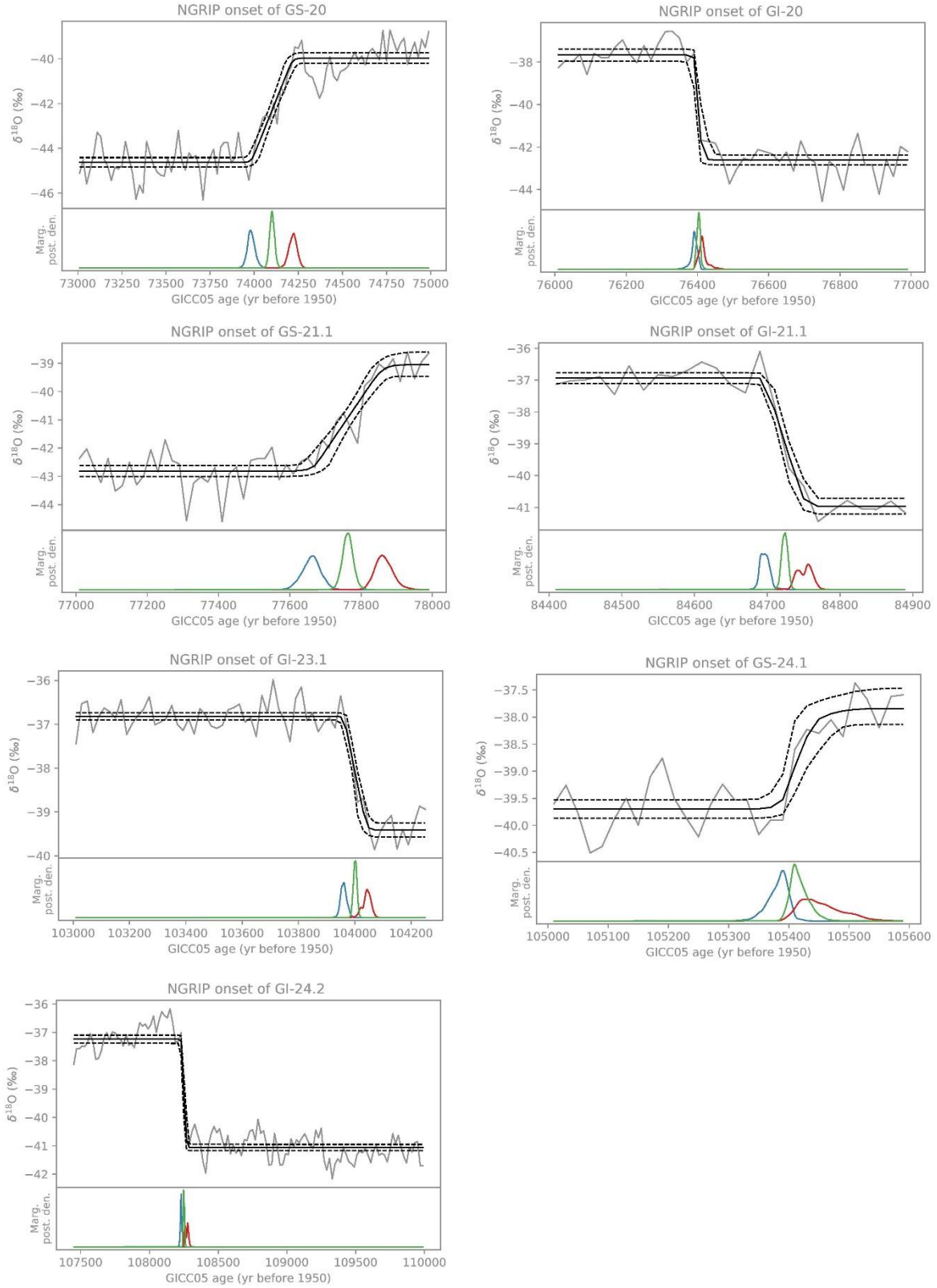


**Figure S7: Fitting results of the Erhardt et al. (2019) algorithm for NGRIP on the GICC05modelext chronology (Wolff et al, 2010). Each of the top panels shows the fitted data together with marginal posterior median and 5th and 95th percentile of the fitted ramp in solid and dashed lines respectively. The bottom panels show the marginal posterior densities for the onset, midpoint and endpoint of the transitions (in red, green and blue).**

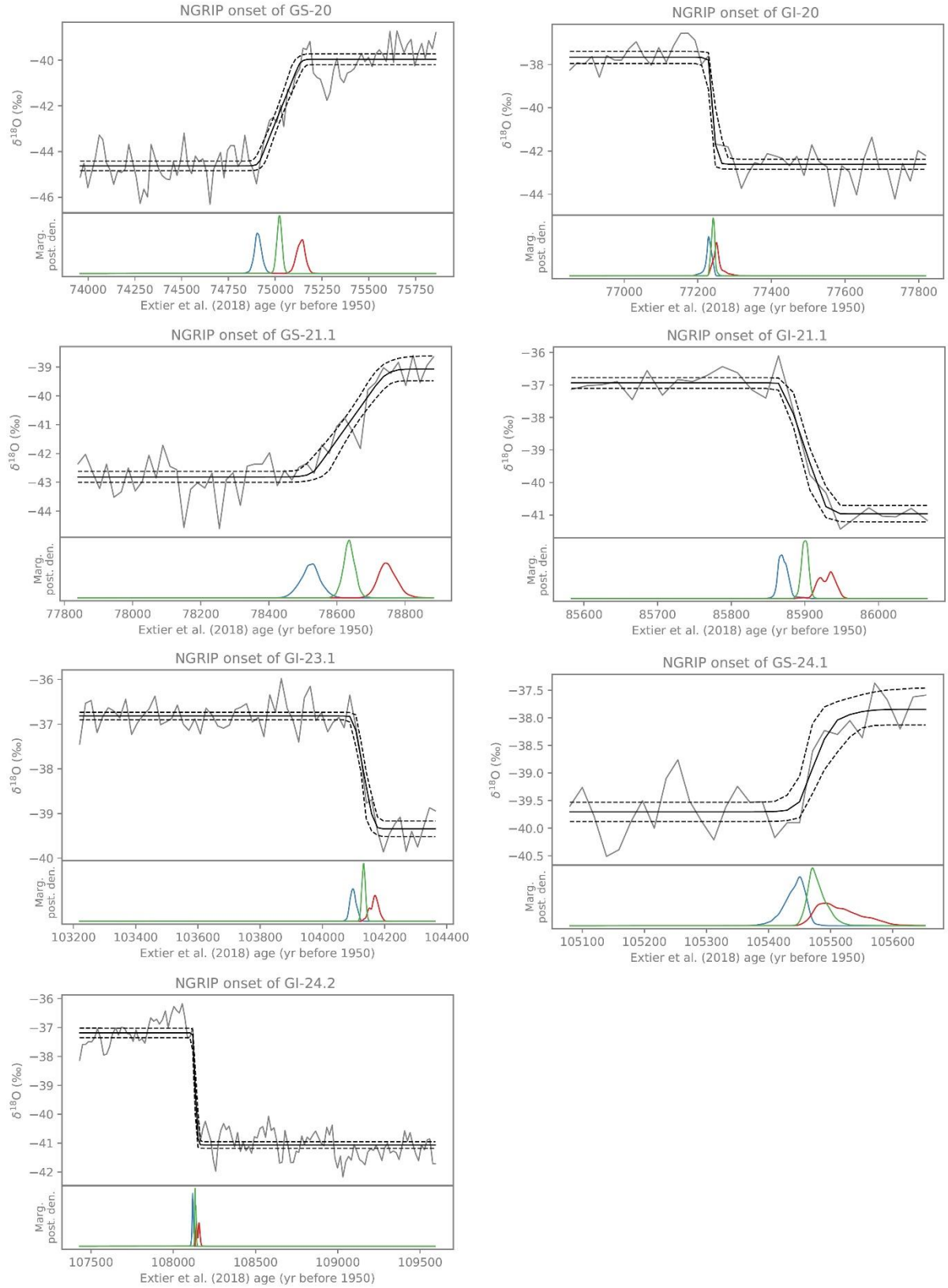


**Figure S7: Fitting results of the Erhardt et al. (2019) algorithm for NGRIP on the Extier et al. (2018) revised AICC2012 chronology. Each of the top panels shows the fitted data together with marginal posterior median and 5th and 95th percentile of the fitted ramp in solid and dashed lines respectively. The bottom panels show the marginal posterior densities for the onset, midpoint and endpoint of the transitions (in red, green and blue).**

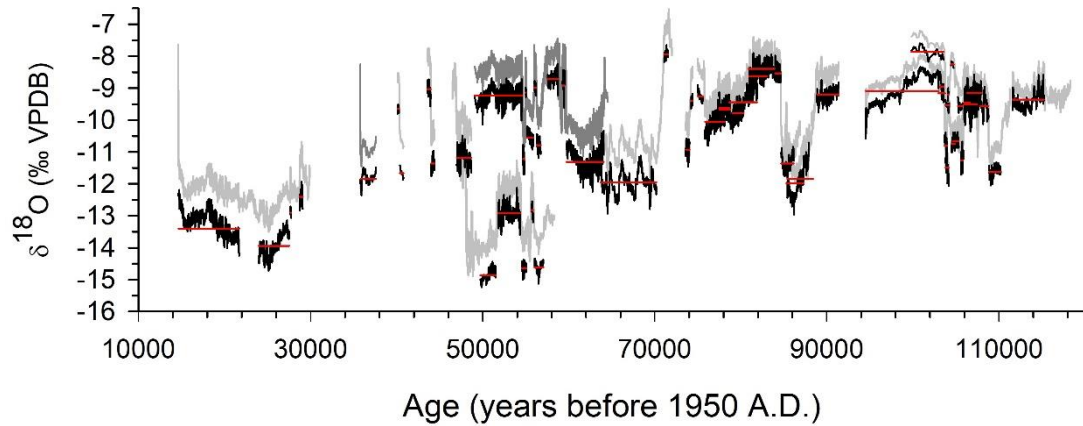


**Figure S8:** Speleothem  $\delta^{18}\text{O}$  records from the northern rim and central European Alps uncorrected for changes in mean  $\delta^{18}\text{O}$  variability of seawater (grey). Light grey are single speleothems, dark grey are composite speleothem records. See Fig. 5 for details of the original data. Sections of the ice-volume-corrected  $\delta^{18}\text{O}$  curve used to establish mean and median  $\delta^{18}\text{O}$  values (black) presented in Table S3. Mean values (red horizontal bars).

**Table S3:** Mean and median  $\delta^{18}\text{O}$  values for specific stadials and interstadials as shown in red horizontal bars (Fig. S8). \*see Fig. S9

Equivalent Stratigraphic Unit	Sample	Longitude	Mean $\delta^{18}\text{O}$	Median $\delta^{18}\text{O}$
GS-2.1	7H3	7.81	-13.4	-13.5
GS-3	7H2	7.81	-13.9	-14.0
GI-3	7H2	7.81	-12.9	-12.8
GI-4	7H2	7.81	-12.4	-12.4
GS-8	HÖL-16/17	10.15	-11.8	-11.8
GI-9	HÖL-7	10.15	-9.65	-9.64
GS-10	HÖL-7	10.15	-11.66	-11.66
GI-11	HÖL-7	10.15	-9.03	-9.01
GS-12	HÖL-7	10.15	-11.36	-11.33
GS-13	HÖL-7	10.15	-11.2	-11.2
GS-14	SPA-49	11.67	-14.9	-14.9
GI-14	HÖL-16/17/18	10.15	-9.2	-9.2
GI-14	SPA-49	11.67	-12.9	-12.9
GS-15.1	HÖL-16/17/18	10.15	-11.2	-11.2
GS-15.1	SPA-49	11.67	-14.6	-14.6
GI-15.1	HÖL-16/17/18	10.15	-9.1	-9.2
GS-15.2	HÖL-16/17/18	10.15	-10.5	-10.5
GI-15.2	HÖL-16/17/18	10.15	-9.0	-9.0
GI-15.2	SPA-49	11.67	-12.8	-12.7
GS-16.1	HÖL-16/17/18	10.15	-10.8	-10.8
GS-16.1	SPA-49	11.67	-14.6	-14.6
GI-16.1	HÖL-16/17/18	10.15	-8.7	-8.7
GI-17.1	HÖL-16/17/18	10.15	-8.9	-8.9
GS-18	HÖL-16/17/18	10.15	-11.3	-11.3
GS-19.2	KC-1	10.11	-12.0	-12.0

GI-19.2	KC-1	10.11	-7.9	-8.0
Equivalent Stratigraphic Unit	Sample	Longitude	Mean $\delta^{18}\text{O}$	Median $\delta^{18}\text{O}$
GS-20	HÖL-19	10.15	-10.9	-10.9
GI-20a	HÖL-19	10.15	-9.4	-9.4
GI-20c	SCH-6	10.07	-9.3	-9.3
GS-21.1	SCH-6	10.07	-10.1	-10.0
GI-21.1a	GAS-12	13.84	-9.5	-9.6
GI-21.1a	GAS-13	13.84	-9.8	-9.7
GI-21.1c	GAS-12	13.84	-9.4	-9.6
GI-21.1c	GAS-13	13.84	-9.8	-9.8
GI-21.1e	BA-7	9.67	-8.4	-8.4
GI-21.1e	BA-1	9.67	-8.6	-8.6
GI-21.1e	GAS-25	13.84	-8.5	-8.6
GS-22	BA-7	9.67	-11.4	-11.4
GS-22	BA-5	9.67	-11.8	-11.8
GS-22	BA-1	9.67	-12.0	-11.9
GI-22	GAS-25	13.84	-9.2	-9.2
GI-23.1	EXC-3	7.78	-8.6	-8.6
GI-23.1	7H12*	7.81	-7.9	-7.8
GI-23.1	HUN-14	12.03	-9.2	-9.2
GI-23.1	GAS-27	13.84	-9.0	-9.0
GS-23.2	7H12*	7.81	-9.5	-9.5
GS-23.2	HUN-14	12.03	-11.5	-11.5
GS-23.2	GAS-27	13.84	-10.8	-10.7
GI-23.2	7H12*	7.81	-8.3	-8.3
GI-23.2	GAS-27	13.84	-9.2	-9.2
GS-24.1	7H12	7.81	-9.6	-9.6
GS-24.1	HUN-14	12.03	-11.3	-11.2
GS-24.1	GAS-27	13.84	-10.7	-10.8
GS-24.1	GAS-29	13.84	-10.7	-10.7
GI-24.1a	GAS-29	13.84	-9.5	-9.4
GI-24.1	EXC-3	7.78	-9.0	-8.9
GI-24.1	HUN-14	12.03	-9.5	-9.5
GI-24.1	GAS-22	13.84	-9.1	-9.1
GI-24.2	EXC-3	7.78	-8.8	-8.8
GI-24.2	HUN-14	12.03	-9.6	-9.6
GS-25	EXC-4	7.78	-12.5	-12.5
GS-25	HUN-14	12.03	-11.6	-11.6
GI-25	SCH-7	10.07	-9.4	-9.4



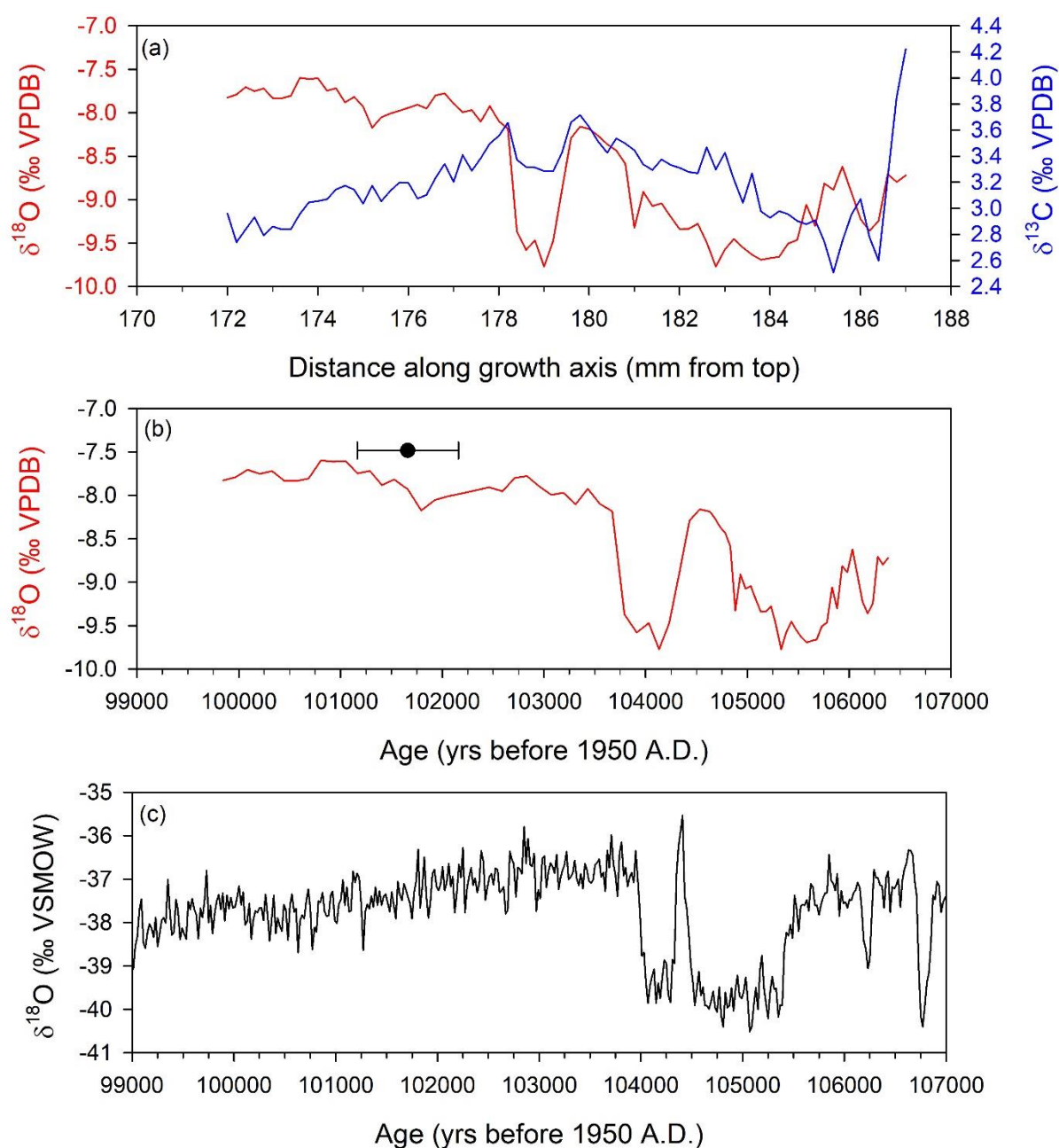


**Figure S9: Preliminary data from Siebenhengste sample 7H12 provided by Marc Luetscher for this study. (a) Stable isotope data relative to distance along growth axis. (b)  $\delta^{18}\text{O}$  on a preliminary age model. The U-Th age (black circle and 2 sigma uncertainty) firmly places the timing in GI-23.1. Since there are no hiatuses, the remainder is matched to a preliminary age model. The quality of the age model is not so important here because we are only interested in the mean  $\delta^{18}\text{O}$  values for the respective stadials and interstadials. (c) NGRIP on GICC05modelext (Wolff et al., 2010).**

## References

- Boch, R., Cheng, H., Spötl, C., Edwards, R. L., Wang, X., and Häuselmann, Ph.: NALPS: a precisely dated European climate record 120–60 ka, *Clim. Past*, 7, 1247–1259, <https://doi.org/10.5194/cp-7-1247-2011>, 2011.
- Cheng, H., Edwards, R. L., Sinha, A., Spötl, C., Yi, L., Chen, S., Kelly, M., Kathayat, G., Wang, X., Li, X., Kong, X., Wang, Y., Ning, Y., and Zhang, H.: The Asian monsoon over the past 640,000 years and ice age terminations, *Nature*, 534, 640–646, <https://doi.org/10.1038/nature18591>, 2016.
- Cheng, H., Edwards, R. L., Shen, C.-C., Polyak, V. J., Asmerom, Y., Woodhead, J., Hellstrom, J., Wang, Y., Kong, X., Spötl, C., Wang, X., and Alexander Jr, E. C.: Improvements in  $^{230}\text{Th}$  dating,  $^{230}\text{Th}$  and  $^{234}\text{U}$  half-life values, and U–Th isotopic measurements by multi-collector inductively coupled plasma mass spectrometry, *Earth Planet. Sc. Lett.*, 371–372, 82–91, <http://dx.doi.org/10.1016/j.epsl.2013.04.006>, 2013.
- Erhardt, T., Capron, E., Rasmussen, S. O., Schüpbach, S., Bigler, M., Adolphi, F., and Fischer, H.: Decadal-scale progression of the onset of Dansgaard–Oeschger warming events, *Clim. Past*, 15, 811–825, <https://doi.org/10.5194/cp-15-811-2019>, 2019.
- Extier, T., Landais, A., Bréant, C., Prié, F., Bazin, L., Dreyfus, G., Roche, D. M., and Leuenberger, M.: On the use of  $\delta^{18}\text{O}_{\text{atm}}$  for ice core dating, *Quaternary Sci. Rev.*, 185, 244–257, <https://doi.org/10.1016/j.quascirev.2018.02.008>, 2018.
- Jaffey, A. H., Flynn, K. F., Glendenin, L. E., Bentley, W. C., and Essling, A. M.: Precision measurement of half-lives and specific activities of  $^{235}\text{U}$  and  $^{238}\text{U}$ , *Phys. Rev. C*, 4, 1889, <https://doi.org/10.1103/PhysRevC.4.1889>, 1979.
- Jiang, X., Wang, X., He, Y., Hu, H.-M., Li, Z., Spötl, C., and Shen, C.-C.: Precisely dated multidecadally resolved Asian summer monsoon dynamics 113.5–86.6 thousand years ago, *Quaternary Sci. Rev.*, 143, 1–12, <https://doi.org/10.1016/j.quascirev.2016.05.003>, 2016.
- Kelly, M. J.: Characterization of Asian Monsoon variability since the Penultimate Interglacial on orbital and sub-orbital timescales, Dongge Cave, China, PhD Thesis, University of Minnesota, USA, 221 pp., 2010.
- Kelly, M. J., Edwards, R. L., Cheng, H., Yuan, D., Cai, Y., Zhang, M., Lin, Y., and An, Z.: High resolution characterization of the Asian Monsoon between 146,000 and 99,000 years B.P. from Dongge Cave, China and global correlation of events surrounding Termination II, *Palaeogeogr. Palaeoclimatol.*, 236, 20–38, <https://doi.org/10.1016/j.palaeo.2005.11.042>, 2006.
- Moseley, G. E., Spötl, C., Svensson, A., Cheng, H., Brandstätter, S., and Lawrence Edwards, R. L.: Multi-speleothem record reveals tightly coupled climate between central Europe and Greenland during Marine Isotope Stage 3, *Geology*, 42, 1043–1046, <https://doi.org/10.1130/G36063.1>, 2014.
- Svensson, A., Andersen, K. K., Bigler, M., Clausen, H. B., Dahl-Jensen, D., Davies, S. M., Johnsen, S. J., Muscheler, R., Parrenin, F., Rasmussen, S. O., Röthlisberger, R., Seierstad, I., Steffensen, J. P., and Vinther, B. M.: A 60 000 year Greenland stratigraphic ice core chronology, *Clim. Past*, 4, 47–57, <https://doi.org/10.5194/cp-4-47-2008>, 2008.
- Veres, D., Bazin, L., Landais, A., Toyé Mahamadou Kele, H., Lemieux-Dudon, B., Parrenin, F., Martinerie, P., Blayo, E., Blunier, T., Capron, E., Chappellaz, J., Rasmussen, S. O., Severi, M., Svensson, A., Vinther, B., and Wolff, E. W.: The Antarctic ice core chronology (AICC2012): an optimized multi-parameter and multi-site dating approach for the last 120 thousand years, *Clim. Past*, 9, 1733–1748, <https://doi.org/10.5194/cp-9-1733-2013>, 2013.
- Wang, Y. J., Cheng, H., Edwards, R. L., Kong, X., Shao, X., Cheng, S., Wu, J., Jiang, X., Wang, X., and An, Z.: Millennial- and orbital- scale changes in the East Asian Monsoon over the past 224,000 years, *Nature*, 451, 1090–1093, <https://doi.org/10.1038/nature06692>, 2008.
- Wedepohl, K. H.: The composition of the continental crust, *Geochim. Cosmochim. Ac.*, 59, 1217–1239, [https://doi.org/10.1016/0016-7037\(95\)00038-2](https://doi.org/10.1016/0016-7037(95)00038-2), 1995.
- Wolff, E. W., Chappellaz, J., Blunier, T., Rasmussen, S. O., and Svensson, A.: Millennial-scale variability during the last glacial: The ice core record, *Quaternary Sci. Rev.*, 29, 2828–2838, <https://doi.org/10.1016/j.quascirev.2009.10.013>, 2010.